Identification of Protein p270/Tpr as a Constitutive Component of the Nuclear Pore Complex–attached Intranuclear Filaments

Volker C. Cordes, Sonja Reidenbach, Hans-Richard Rackwitz, and Werner W. Franke

Division of Cell Biology, German Cancer Research Center, D-69120 Heidelberg, Federal Republic of Germany

Abstract. Using a monoclonal antibody, mAb 203-37, we have identified a polypeptide of M_r ~270 kD (p270) as a general constituent of the intranuclear filaments attached to the nucleoplasmic annulus of the nuclear pore complex (NPC) in diverse kinds of vertebrate cells. Using cDNA cloning and immunobiochemistry, we show that human protein p270 has a predicted molecular mass of 267 kD and is essentially identical to the coiled-coil dominated protein Tpr reported by others to be located on the outer, i.e., cytoplasmic surface of NPCs (Byrd, D.A., D.J. Sweet, N. Pante, K.N. Konstantinov, T. Guan, A.C.S. Saphire, P.J. Mitchell, C.S. Cooper, U. Aebi, and L. Gerace. 1994. *J. Cell Biol.* 127: 1515–1526). To clarify this controversial localization, we have performed immunoelectron microscopy in diverse kinds of mammalian and amphibian cells with a series of antibodies raised against different epitopes of human and *Xenopus laevis* p270/Tpr. In these experiments, the protein has been consistently and exclusively detected in the NPC-attached intranuclear filaments, and p270/Tpr-containing filament bundles have been traced into the nuclear interior for up to 350 nm. No reaction has been noted at the cytoplasmic side of NPCs with any of the p270/Tpr antibodies, whereas control antibodies such as those against protein RanBP2/Nup358 specifically decorate the cytoplasmic annulus of NPCs. Pore complexes of cytoplasmic annulate lamellae in various mammalian and amphibian cells are also devoid of immunodetectable protein p270/Tpr. We conclude that this coiled-coil protein is a general and ubiquitous component of the intranuclear NPC-attached filaments and discuss its possible functions.

Nuclear pore complexes (NPCs)[1] are constitutive structures of the nuclear envelope in all eukaryotic cells and represent gateways between the cytoplasm and the nucleus through which the exchange and bidirectional transport of molecules and particles takes place (for reviews see, e.g., Rout and Wente, 1994; Davis, 1995; Pante and Aebi, 1995*b*). These structures are large assemblies (110–145 MDa in vertebrates) of globular and fibrillar substructures arranged in an eightfold rotational symmetry (Franke, 1966, 1970; Gall, 1967; Reichelt et al., 1990; Hinshaw et al., 1992; Akey and Rademacher, 1993; for review see Pante and Aebi, 1995*a*) and estimated to be composed of ~60–100 different proteins. In vertebrates, NPC proteins molecularly characterized include the transmembrane proteins gp210 (Gerace et al., 1982; Wozniak et al., 1989) and Pom 121 (Hallberg et al., 1993) and at least ten nonmembranous "nucleoporins," some of which represent components of NPC-associated filamentous structures (for recent review see Bastos et al., 1995).

Attached to the cytoplasmic annular rim of the NPC are short (25–50-nm) filaments that contain not only the initial binding sites for transport factors involved in nuclear protein import (Richardson et al., 1988; Newmeyer and Forbes, 1988; Melchior et al., 1995; Wu et al., 1995; for reviews see, e.g., Sweet and Gerace, 1995; Melchior and Gerace, 1995; Simos and Hurt, 1995; Pante and Aebi, 1996) but also intracellular "docking" sites for certain DNA viruses (e.g., Summers, 1971; Chardonnet and Dales, 1972). Structural components of these NPC-attached cytoplasmic filaments include the putative oncoprotein CAN/Nup 214 (Kraemer et al., 1994) and the recently identified Ran protein-binding nucleoporin RanBP2/Nup358 (Yokoyama et al., 1995; Wu et al., 1995; Wilken et al., 1995). Protein Tpr (translocated promotor region), whose gene has been implicated in the activation of the protooncogenes *met*, *raf*, and *trk* (Park et al., 1986; Soman et al., 1991; Greco et al., 1992), has also been reported to be exclusively located in the NPC-attached cytoplasmic fibrils (Byrd et al., 1994) and is considered to contribute to the formation of these filaments.

At the other, nucleoplasmic side, bundles of filaments of ~5 nm diam appear to be anchored at the NPC and often extend into the nuclear interior for various lengths, in am-

Address all correspondence to Volker C. Cordes and Werner W. Franke, Division of Cell Biology, German Cancer Research Center, Im Neuenheimer Feld 280, D-69120 Heidelberg, FRG. Tel.: (49) 6221-423400. Fax: (49) 6221-423404.

1. *Abbreviations used in this paper*: aa, amino acid; CMV, cytomegalovirus; ECL, enhanced chemiluminescence; KLH, keyhole limpet hemocyanin; NPC, nuclear pore complex; TBST, TBS containing 0.05% Tween-20.

phibian oocytes for >300 nm. These NPC-attached nuclear filament bundles are symmetrically arranged and appear to form a cylinder (Franke, 1970; Franke and Scheer, 1970*a*,*b*; Kartenbeck et al., 1971; Richardson et al., 1988; Ris and Malecki, 1993) built on a specific NPC-proximal filamentous array only ~30–70 nm in length that has been described as a "fish trap," "cage," or "basket" (Ris, 1989, 1991; Jarnik and Aebi, 1991; Goldberg and Allen, 1992). The functions of both the long and the short (fish trap) intranuclear filament arrays are unknown. Proteins localized to the nucleoplasmic side of the NPC at distances either more proximal or more distal to the inner annulus include p97/Nup98 (Radu et al., 1995; Powers et al., 1995) and Nup153 (Sukegawa and Blobel, 1993; see also Cordes et al., 1993; Pante et al., 1994). Of these, protein Nup153 has been reported to occur in both the long and the short intranuclear filaments (Cordes et al., 1993; Pante et al., 1994).

In the course of our attempts to elucidate the composition and assembly of the NPC-attached intranuclear filament bundles, we have identified in amphibians and mammals a protein component of ~270 kD molecular mass that turned out to be protein Tpr, localized exclusively and constitutively to these intranuclear filaments, much to our surprise and at variance with previous reports (Byrd et al., 1994; Bangs et al., 1996).

Materials and Methods

Cell Cultures

Culture conditions for cells of human lines HeLa, glioma U333/CG/343 MG, PLC, A-431, CaCo2, HF-SV80, MCF-7, and HaCaT; for bovine lines BMGE+H clone 5 and MDBK; for canine MDCK, porcine PK(15), African green monkey RC37, marsupial PtK2, and rodent RV; and for primary cultures of human umbilical cord endothelial cells have been described in detail (Cordes et al., 1996). Murine fibroblasts of lines L-M(TK $^-$) (American Type Culture Collection code ATCC CCL 13) and 3T3-L1 (ATCC CCL 92.1) were grown in DME (ICN Biomedicals, Costa Mesa, CA) supplemented with 10% FCS, and rat hepatoma cells of line Faza 967-D2 (Venetianer et al., 1983) were grown in Ham's F12 medium (Boehringer Mannheim GmbH, Mannheim, FRG). *Xenopus laevis* kidney epithelial cells of line A6 (ATCC CCL 102) were grown at 28°C in DME with 10% FCS and diluted with 15% H_2O.

Tissues

Tissues were frozen in isopentane cooled with liquid nitrogen to −140°C, and then stored at −70°C. Human tissues (cerebrum, fetal cerebellum, colon and colon carcinoma, epidermis, erythroblastoma, liver, esophagus, ovary, smooth muscle, and testis) were kindly provided by Dr. Roland Moll (Department of Pathology, Martin Luther-University, Halle-Wittenberg, FRG). Bovine tissues (liver, testis, calf thymus) were obtained from the slaughter house. South African clawed frogs (*Xenopus laevis*) were bred in this institute, and pieces of skin, ovary, and liver were obtained by surgery as described (Cordes et al., 1995).

Antibodies

mAb 203-37 (Matritech, Cambridge, MA) against the nuclear matrix fraction from cultured cells of breast cancer line T-47D (see, however, Bangs et al., 1996 for a similar mAb) and mAb 414 (BAbCO, Richmond, CA) against the XFXFG motif–containing domain common to some nucleoporins (Davis and Blobel, 1986; Sukegawa and Blobel, 1993) have been obtained commercially. mAb X167 against lamins A/C (Höger et al., 1991), rabbit and guinea pig antibodies to RanBP2/Nup358 (rb-αRBP2-2, gp-αRBP2-2; Cordes et al., 1996), and guinea pig antibodies against nucleolar protein NO38 were from this institute (kindly provided by Dr. Marion Schmidt-Zachmann, German Cancer Research Center, Heidelberg). Guinea pig antibodies to lamin A were a gift of Dr. Georg Krohne (University of Würzburg, FRG).

To raise antibodies against synthetic peptides of human and *Xenopus* Tpr, putative antigenic sites of this protein with high degrees of surface probability were determined by the algorithms of Jameson and Wolf (1988) and Emini et al. (1985) and controlled for low homology with other proteins by sequence database searches. Peptides were synthesized by t-Boc chemistry (Schnölzer et al., 1992) and coupled via a carboxy-terminal cysteine residue to maleimide-activated keyhole limpet hemocyanin (KLH; 1 mg peptide/1 mg KLH), using the Imject Activated Immunogen Conjugation Kit (Pierce Europe, Oud-Beijerland, The Netherlands). Human Tpr peptides correspond to amino acids (aa) 1,622–1,640 (hTpr-Pep1: ERHLEQRDEPQEPSNKVPE) and aa 2,063–2,084 (hTpr-Pep2: SERQAPRAPQSPRRPPHPLPPR) of the 2,363-aa Tpr sequence presented below. The *Xenopus* Tpr peptide (QHFFDEEDRTVPSTPT), deduced from the partial DNA sequence (see below), is homologous to aa 2,124–2,139 of human Tpr. For the first injection, the KLH-coupled peptides were emulsified with an equal volume of complete Freund's adjuvant and, for the booster injections, with incomplete adjuvant. Guinea pigs (hTpr-Pep1 and 2; xlTpr-Pep3) and rabbits (hTpr-Pep2; xlTpr-Pep3) were immunized four times subcutaneously with 70–100 μg protein per injection. Booster injections were at days 14 (21), 35 (42), and 70. Guinea pigs were killed at ~day 82. Rabbits were held for longer periods and occasionally reboostered. Blood was collected in vacutainer SST-tubes (Becton-Dickinson, Heidelberg, FRG). For affinity chromatography, peptides containing the antigenic determinants were coupled to Ultra Link Iodoacetyl on 3 M Emphaze Biosupport Medium AB1 (Pierce Europe). The peptide–resin was first mixed with 1% BSA in PBS by rotation for 30 min, washed with 20 vol of PBS, and then mixed for 90 min at 4°C with 10 vol of sera, diluted 1:3 in PBS. After washings with 20 vol each of PBS and 10 mM sodium phosphate (pH 6.8), antibodies were eluted in fractions of 400 μl with 100 mM glycine-HCl (pH 2.3) and immediately neutralized with ~0.04 vol of 1 M Tris-HCl (pH 9.5). Purified antibodies, supplemented with an equal volume of glycerol or 0.25 vol PBS with 20% BSA, and 0.03% NaN_3, were stored at −70°C.

Cell Fractionation

During the entire fractionation procedure, cultured cells grown to near confluency (70–80%) remained in the petri dishes (10 cm diam). After briefly washing the cells twice with hand-warm PBS containing 2 mM $MgCl_2$ and once with MOPS buffer (50 mM MOPS-NaOH, pH 7.0, 1 mM EGTA, 5 mM $MgCl_2$, and 0.75% vol/vol of saturated PMSF in ethanol) at room temperature, all subsequent steps were performed at ~4°C using ice-cold solutions. Solutions pipetted onto the cells were recollected after each fractionation and washing step and were immediately centrifuged at 4°C for 4 min at 13,000 *g*. The resulting supernatants were combined with 4 vol of ice-cold methanol, and proteins were allowed to precipitate overnight at −20°C. Cells were first extracted in 2 ml MOPS buffer containing 0.2% Triton X-100 for 5 min by mildly and briefly shaking the petri dishes every 30–60 s, briefly washed with 2 ml MOPS buffer, and then extracted for 5 min in 2 ml MOPS containing 0.5 M NaCl, again followed by a brief washing with 2 ml MOPS. The residual cyto- and karyoskeletons that remained attached to the dishes were immediately scraped off in 0.5 ml of 90°C SDS sample buffer and boiled. For digitonin permeabilization, cells on dishes were incubated for 5–10 min in 2 ml ice-cold PBS containing 0.005% digitonin without protease inhibitors, and then washed with 2 ml PBS. Soluble proteins in the digitonin and washing solutions were combined, cleared by centrifugation, and precipitated from the supernatant with methanol. The permeabilized cells were boiled in SDS sample buffer.

The manual isolation of stage VI nuclei from *Xenopus laevis* oocytes has been described elsewhere (Cordes et al., 1995).

Gel Electrophoresis and Immunoblotting

SDS-PAGE of proteins was by the method of Thomas and Kornberg (1975). For two-dimensional gel electrophoresis, IEF (O'Farrell, 1975) was used in the first dimension, and SDS-PAGE in the second (Laemmli, 1970). After electroblotting of proteins onto nitrocellulose, the filters were preincubated for at least 2 h in Tris-buffered saline containing 0.05% Tween-20 (TBST) and 5% milk powder (TBST-milk). Incubation with primary antibodies was for 2 h. Filter washings were usually performed with TBST. In some experiments, more stringent washing conditions were applied, using PBS containing 0.1% Triton X-100 and PBS with additional 0.4 M NaCl, i.e., the same stringency conditions as later applied for cDNA

library screening (see below). Bound antibodies were detected by HRP-coupled secondary antibodies (Dianova, Hamburg, FRG) applying the enhanced chemiluminescence (ECL) method (Amersham, Braunschweig, FRG). To remove bound antibodies, filters were shaken for 3 × 30 min in 0.1 M glycine-HCl (pH 2.6) containing 20 mM magnesium acetate and 50 mM KCl. Filters were then washed in TBST and shaken in TBST-milk for 1 h before reincubation with antibodies.

Isolation of cDNA Clones and PCR Products

The monoclonal IgG1 antibody 203-37, the antigen of which has not been known by the producer (Matritech) at the beginning of this study, was used to screen 1.2×10^6 plaques of a human fetal brain UNI-ZAP™ XR cDNA library (Stratagene, La Jolla, CA). After plaque transfer onto isopropylthio-β-D-galactosidase–treated nitrocellulose, filters were washed in TBST and saturated in TBST-milk. Incubation with mAb 203-37 in TBST-milk was followed by washings in TBST, PBS with 0.1% Triton X-100, and PBS with additional 0.4 M NaCl. Filters were then incubated with HRP-coupled secondary antibodies, again followed by stringent washings. Immunoreactive clones were identified by ECL. Subcloning of pBluescript phagemids by in vivo excision was performed as described in the Stratagene protocol.

PCR was performed using a *Xenopus laevis* kidney UNI-ZAP™ XR cDNA library (Stratagene) as template. PCR was carried out in 50 μl total vol containing 320 ng DNA template, 10 pmol of each sense and antisense primers, and 2 U Taq polymerase per reaction. Cycling conditions were as follows: (1) cycle: 5 min at 95°C; 1 min at 55°C; 2 min at 72°C. (2–34) cycle: 2 min at 92°C; 1 min at 55°C; 2 min at 72°C. The end of cycle 34 was followed by 10 min at 72°C. Sense primers were initially deduced from a GenBank sequence (accession number U12646) that had been entered as a noncoding region of an unpublished *Xenopus laevis* integrin variant. Sequence comparison with human protein Tpr, however, indicated that this DNA segment encoded partial aa sequences of the *Xenopus* Tpr protein; all three forward frames of the entered DNA sequence encoded short aa sequence stretches with apparent homology to human protein Tpr. As antisense primer for the first set of PCRs performed, the T7 primer (Stratagene) was used; its binding site on the Uni-ZAP™ XR vector flanks the unidirectionally cloned cDNA inserts at their 3′-end. Other primers were also deduced from PCR product sequences (see below). PCR assays were generally performed without using PCR-amplified DNA from other reactions as intermediate template from which to proceed. PCR products corresponding to a given DNA segment were obtained in at least two independent reactions and sequenced. Several overlapping DNA fragments were assembled into a DNA sequence of 1,811 bp that encoded 558 aa of the *Xenopus* Tpr protein. Corresponding to this nucleotide numbering, primer positions were as follows: 1–18, 937–957, 1137–1117, 1164–1146. Dideoxy sequencing of cDNAs and PCR products was according to Sanger et al. (1977).

In Vitro Translation and Immunoprecipitation

In vitro transcription–translation of the human Tpr protein cDNA clone T1 was performed at 30°C for 90 min in the presence of [^{35}S]methionine, using the coupled reticulocyte lysate system and T3 RNA polymerase (Promega, Heidelberg, FRG).

For immunoprecipitation, 25 μl of PBS-washed, preswollen protein G–Sepharose was suspended in 200 μl PBS containing 10 μl mAb 203-37, then mixed for 1 h by rotation at 4°C, and subsequently washed four times with 1.5 ml PBS. In parallel, 25 μl reticulocyte lysate containing the [^{35}S]labeled in vitro translation products was diluted with 200 μl PBS and mixed for 1 h by rotation at 4°C with another 25-μl aliquot of PBS-washed, preswollen protein G–Sepharose; the beads were then pelleted by centrifugation. The resulting reticulocyte lysate supernatant, containing the [^{35}S]labeled Tpr polypeptides, was transferred to the aliquot of protein G–Sepharose with mAb 203-37, whereas proteins unspecifically bound to the beads after two washings with PBS were released by boiling in SDS sample buffer and later analyzed by SDS-PAGE for control. Protein G–Sepharose with mAb 203-37 and reticulocyte lysate supernatant were mixed by rotation for 1 h at 4°C; the beads were then pelleted and washed five times in PBS. Bound proteins were released by boiling in SDS sample buffer and analyzed by SDS-PAGE.

DNA Transfection

The entire cDNA fragment of clone T1 representing mRNA encoding full-length human protein Tpr was isolated by NotI/ApaI or NotI/Bsp102I digestion and subcloned into eukaryotic expression vector pRC/CMV containing a cytomegalovirus (CMV) promoter (Invitrogen, San Diego, CA) and expression vector p163/7, containing a major histocompatibility complex (MHC) class I H-2 promoter. p163/7 is identical to p164/7 (Niehrs et al., 1992) with the exception of an inverted multiple cloning site. Using plasmid DNA purified on Quiagen Matrix Columns (Diagen, Hilden, FRG), cells were transfected by the calcium phosphate precipitation method as described (Leube et al., 1994).

Immunofluorescence Microscopy

Tissue cryostat sections were fixed either in acetone or with formaldehyde before incubation with antibodies (Cordes et al., 1995). Cultured cells were fixed with methanol/acetone (Cordes et al., 1993) or in 2% formaldehyde in PBS (20 min). After aldehyde fixation, cells were washed with PBS containing 50 mM NH_4Cl, followed by two washes in PBS, permeabilized by 0.1% Triton X-100 in PBS for 3 min, and again washed twice in PBS. In some experiments, cells were only permeabilized with 0.004% digitonin (Sigma, Deisenhofen, FRG) in PBS at 4°C for 4 min, washed in ice-cold PBS, and fixed in 2% formaldehyde in PBS (20 min). Incubations with primary antibodies were for 30 min; incubations with secondary antibodies coupled to Texas red sulfonyl chloride, FITC, cyanine 2-OSu bisfunctional or cyanine 3.29-OSu (Biotrend, Cologne, FRG; or Dianova) were between 15 and 30 min. Washings were usually in PBS, but in some experiments, PBS containing 0.1% Triton X-100 and PBS with additional 0.4 M NaCl were used. For double-labeling experiments, cells were first incubated with a mixture of antibodies from two different species, and then incubated with the corresponding secondary antibodies. Affinity-purified secondary antibodies specifically used for double labelings (Biotrend) were controlled to exhibit no cross-reactivity to the primary antibodies of the respective other species. Samples were analyzed in a Zeiss Axiophot (Zeiss, Oberkochen, FRG) and photographed on TMY films (Eastman Kodak Co., Rochester, NY).

Immunolocalization by EM

Tissue cryostat sections (5 or 10 μm in thickness) were either fixed with 2% formaldehyde, followed by washes in PBS containing 50 mM NH_4Cl, or by treatment with −20°C acetone (see above). For immunoelectron microscopy on formaldehyde-fixed cultured cells, these were permeabilized with 0.005% digitonin in PBS for 10 min. Before the addition of antibodies, samples were kept for 15 min in blocking solution (PBS with 5% goat serum, 0.1% cold water fish gelatine, and 5% BSA), and then washed twice for 5 min each in PBS with 1% BSA or 0.1% acetylated BSA (BSA-c; Biotrend). All subsequent incubations with antibodies and washings in PBS were in the presence of 1% BSA or 0.1% BSA-c. Incubations with primary antibodies were for 2 h, and with secondary antibodies coupled to 5- or 10-nm colloidal gold grains (Biotrend or Amersham) either for 2 h or overnight. Control experiments, using gold-coupled secondary antibodies alone or together with preimmune sera from Tpr-immunized animals, were carried out in parallel under identical conditions and statistically evaluated. Nonspecific binding of gold grains to NPCs (see Feldherr, 1974) was greatly reduced by the blocking agents applied and usually ranged below 1–2%. Gold-labeled secondary antibodies used for double labelings were controlled to exhibit only minor cross-reactivity to the primary antibodies of the respective other species. After washes in PBS, sections were fixed with 2.5% glutaraldehyde, postfixed with 2% aqueous OsO_4, dehydrated, and embedded in Epon 812 as described (Cordes et al., 1995).

Manually isolated nuclei of *Xenopus* oocytes isolated in 5:1 buffer (Cordes et al., 1995) were immediately transferred into ice-cold PBS containing 2% formaldehyde. After 25 min of fixation, the nuclei were washed twice with PBS containing 50 mM NH_4Cl, and then incubated in PBS with 0.1% BSA-c and 5% goat serum. In this solution each nucleus was ruptured with a pair of tweezers, and the perforated nuclei were then gently pelleted by a 5-min centrifugation at 2,000 *g*, resulting in a very loose pellet. Approximately 90% of the blocking solution was drawn off and replaced by PBS with 0.1% BSA-c, thereby resuspending the nuclei. All subsequent incubations and washings were in PBS with 0.1% BSA-c. Nuclei were first incubated with primary antibodies for 2–3 h, washed four times, with intermediate 3-min centrifugations at 2,000 *g*, and then incubated with gold-coupled secondary antibodies for 12 h. All subsequent steps leading to embedding of nuclei in Epon 812 were as described (Cordes et al., 1995).

Results

Identification of a 270-kD Mammalian Protein as a Novel Component of NPC-attached Intranuclear Filaments

mAb 203-37 showed in immunofluorescence microscopy of cultured cells, permeabilized either by methanol/acetone treatment or by use of Triton X-100 after initial formaldehyde fixation, a punctate staining in the nuclear periphery, similar to that obtained by immunostainings of NPCs. Positive cells included diverse human cell types differing in differentiation such as cervix adenocarcinoma cells of line HeLa (Fig. 1, *a* and *a′*), glioblastoma cells U333/CG/343 MG, primary cultures of endothelial cells, hepatocellular carcinoma PLC cells, carcinoma cells of line A-431, colon adenocarcinoma CaCo2 cells, SV-40–transformed fibroblasts ("SV-80 cells"), and keratinocytes of line HaCaT (not shown), demonstrating that the antigen was widespread if not ubiquitous. Bovine mammary gland epithelial BMGE cells (Fig. 1 *b*) and kidney cells of line MDBK (not shown), porcine kidney cells of line PK(15) (Fig. 1 *c*), and canine MDCK cells (not shown) were also immunoreactive with this mAb. In some cell cultures, occasional intranuclear speckles were noticeable in addition to the peripheral staining (see also below). Nuclear immunostaining was not observed in rat cells of lines RV and 967-D2, murine cells of lines L-M(TK$^-$) and 3T3, marsupial PtK2 cells, and African green monkey cells of line RC37. *Xenopus laevis* kidney epithelial cells of line A6 were also negative.

When cells were permeabilized with 0.004% digitonin, striking differences of nuclear labeling were noticed when comparing mAb 203-37 with antibodies against RanBP2/Nup358, a nucleoporin located at the cytoplasmic side of the NPC. While RanBP2 antibodies showed nuclear labeling in all cells, indicating full accessibility of this protein, mAb 203-37 stained only nuclei of some cells while others were negative (not shown). Moreover, double-label immu-

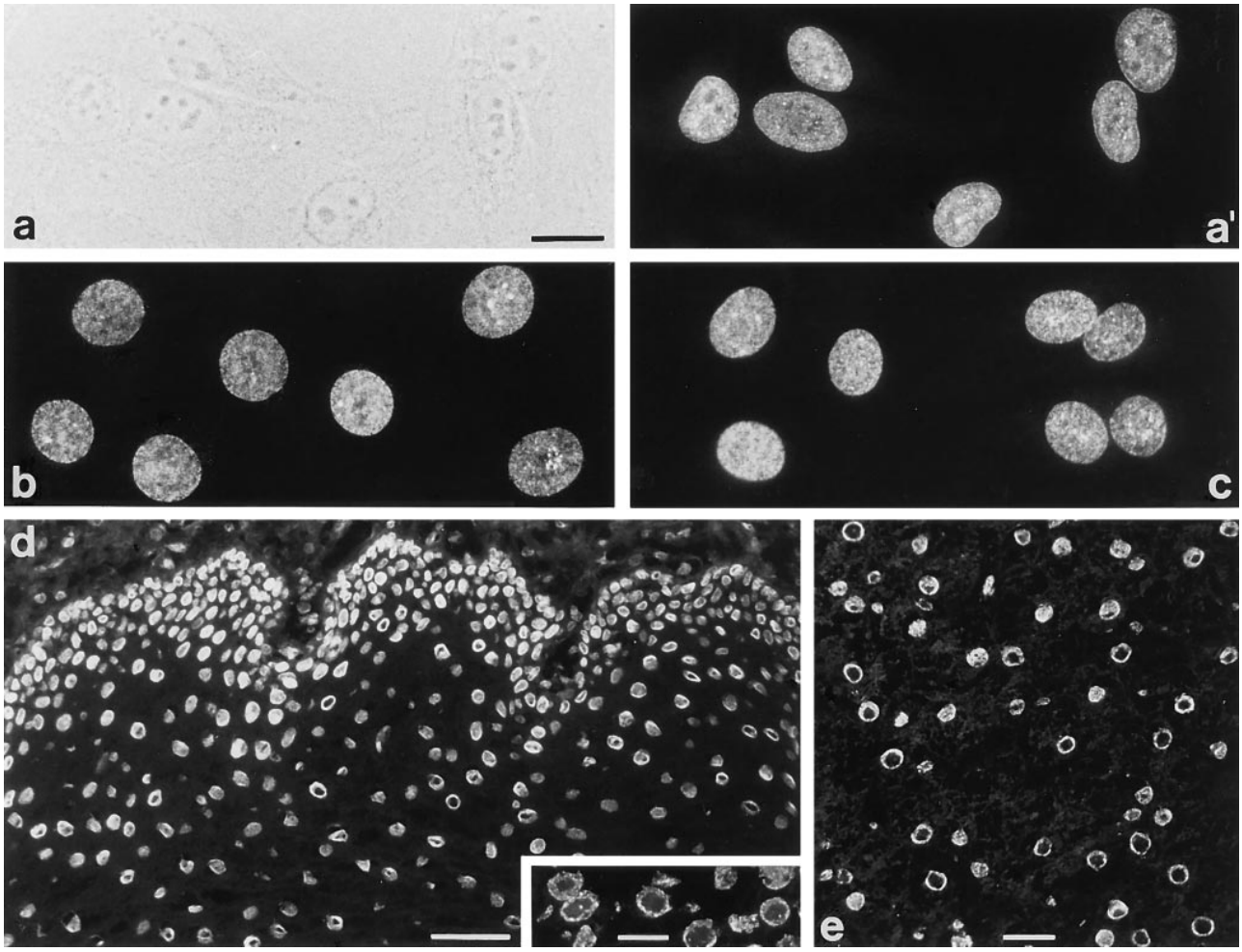

Figure 1. Immunofluorescence microscopy of cultured mammalian cells and tissue cryostat sections after reaction with mAb 203-37. (*a*) Phase contrast and (*a′*) epifluorescence optics of human adenocarcinoma cells of line HeLa. (*b–e*) Epifluorescence optics of cultured bovine mammary gland epithelial cells of line BMGE (*b*), porcine kidney cells of line PK(15) (*c*), and cryostat sections of human esophagus (*d*), human testis (*inset*), and bovine liver (*e*). The finely punctate nuclear labeling in cultured cells is reminiscent of NPC staining. In a minor proportion of cells additional intranuclear dot-like structures are observed (*a′*, *b*, and *c*). Tissue cryostat sections (*d* and *e*) reveal staining of the nuclear periphery and also occasional intranuclear dots (see *inset* in *d*). Cells were fixed either with methanol/acetone (*a*, *a′*, and *c*) or with formaldehyde followed by detergent treatment (*b*) before incubation with antibodies. Cryostat sections were fixed with formaldehyde without subsequent detergent treatment. Bars: (*a*, *inset* in *d* and *e*) 20 μm; same magnification in *a–c*; (*d*) 50 μm.

nofluorescence microscopy using antibodies against nucleolar and lamin proteins further showed that the antigen recognized by mAb 203-37 is accessible only in a specific proportion of nuclei in which intranuclear structures such as the lamina and the nucleolus were also labeled. This indicated that the mAb 203-37 antigen is also intranuclear.

Immunofluorescence microscopy performed on cryostat sections of human and bovine tissues confirmed immunolabeling in the nuclear periphery with mAb 203-37 in all tissues examined, including human esophagus (Fig. 1 *d*), testis (Fig. 1 *d*, *inset*), ovary, liver, skin, smooth muscles, cerebrum, fetal cerebellum, erythroblastoma, and colon carcinoma (not shown), as well as bovine liver (Fig. 1 *e*), testis, and thymus (not shown). In most tissues, we observed occasional intranuclear dot reactions in addition to the nuclear rim staining (an example is shown in Fig. 1 *d*, *inset*).

To identify the antigen recognized by mAb 203-37, we performed immunoblotting on total cell proteins of HeLa cells and identified a protein of M_r ~270 kD (Fig. 2, *a* and *a′*), henceforth called p270. Cell fractionation revealed that p270 remained structure associated after cell extractions with detergent and intermediate salt concentrations (Fig. 2, *b* and *b′*). Immunoreactive polypeptides of lower molecular weight, detected in fractions representing salt-extracted soluble proteins (Fig. 2 *b′*, lane *3*), were considered to be degradation products of p270. Indeed, fractionation of cells induced proteolytic degradation of p270 and omission of protease inhibitors, and prolonged fractionation procedures resulted in an increase of lower molecular weight polypeptides reactive with mAb 203-37. Protein p270 was also identified by immunoblottings with mAb 203-37 on total cell proteins of porcine PK(15) and bovine BMGE cells (Fig. 2, *c* and *c′*), as well as canine MDCK cells (not shown), whereas rodent and marsupial p270 did not cross-react with this antibody. Immunoblottings on African green monkey proteins yielded a weak reaction signal after prolonged exposure (not shown). In essence, our immunoblotting results confirm and extend the study of Bangs et al. (1996) performed largely in parallel.

To localize p270 at the EM level, we examined its distribution by preembedding immunogold localization using mAb 203-37 and 5-nm gold–coupled secondary antibodies on cryostat sections of human and bovine tissues and on monolayers of detergent-permeabilized human PLC cells (Fig. 3, *a–f*). Specific labeling was found on intranuclear filamentous structures that appeared to be attached to NPCs. In some sections, such gold particle–decorated filament bundles projected into the nuclear interior for up to 200 nm (see, e.g., Fig. 3, *b* and *c*). Double immunogold labeling with antibodies against protein RanBP2/Nup358 (10-nm gold–coupled secondary antibodies) and mAb 203-37 (5-nm gold) showed that both margins of the NPC were accessible, and thus confirmed the specificity of the intranuclear localization of p270 (Fig. 3, *g–j*). Besides this labeling of NPC-attached intranuclear filaments, we occasionally also noticed specific mAb 203-37 labeling of unknown intranuclear spheroidal structures ~40–200 nm in diam that were located at greater distances from the nuclear envelope (see below).

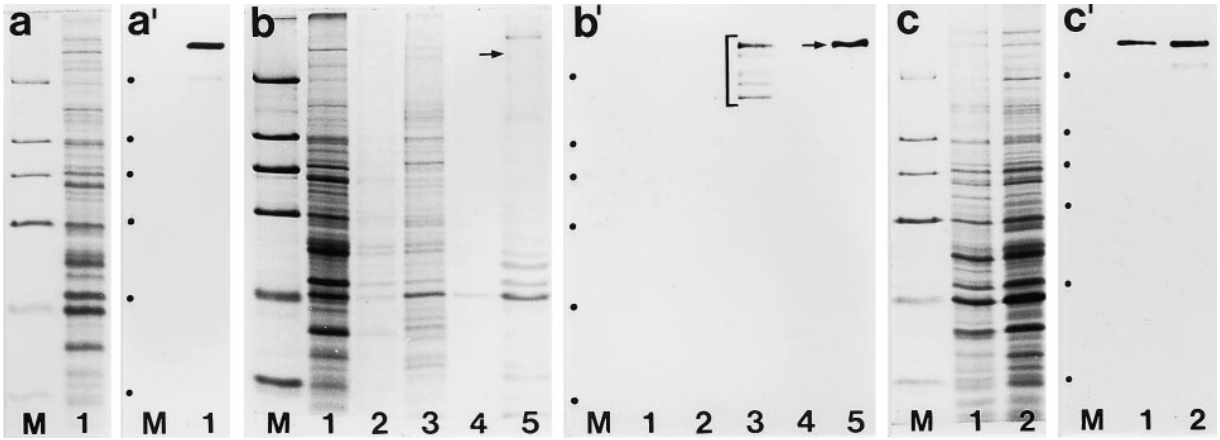

Figure 2. Immunoblot detection of a ~270-kD mammalian protein reactive with mAb 203-37. Proteins were separated by SDS-PAGE and then, in parallel, either stained by Coomassie blue (*a*, *b*, and *c*) or transferred to nitrocellulose filters for immunodetection of proteins (*a′*, *b′*, and *c′*) by enhanced chemiluminescence reaction (ECL). Same amounts of protein were loaded in corresponding lanes of gels for Coomassie staining and immunoblotting. (*a*) Separation of total proteins from HeLa cells and (*a′*) immunoblot detection of a ~270-kD protein, p270, immunoreactive with mAb 203-37. (*b* and *b′*) Fractionation of HeLa cells and immunoblot detection of p270 in a residual detergent and salt-resistant fraction: Hela cells were first extracted with 0.2% Triton X-100 (lanes *1*), washed with detergent-free buffer (lanes *2*), extracted with 500 mM NaCl (lanes *3*), and washed with nearly salt-free buffer (lanes *4*). The residual cyto- and karyoskeletal proteins were separated in lanes *5*. Gels were loaded with the same percentage of proteins from each fraction. Note that the major proportion of p270 remains structure-associated after detergent and intermediate ionic strength-salt treatment. A certain amount of intact p270 has been released into solution by salt extraction as well as putative degradation products (marked by a bracket in *b′*). In contrast to protein p270, a weakly immunoreactive polypeptide of ~75 kD, visible after prolonged film exposure (not shown) in the residual cyto- and karyoskeletal fraction (lane *5*), was not detected after application of more stringent filter washing conditions (see Materials and Methods). (*c* and *c′*) Separation of total proteins from porcine kidney cells of line PK(15) (lanes *1*) and bovine mammary gland epithelial cells of line BMGE (lanes *2*) and immunoblot detection of protein p270 with mAb 203-37 also in these species. Relative molecular masses of marker proteins (*M*) in *a–c* (denoted by dots at the left margin in *a′*–c′) are, from top to bottom, as follows: 205, 116, 97, 66, 45, and 29 kD.

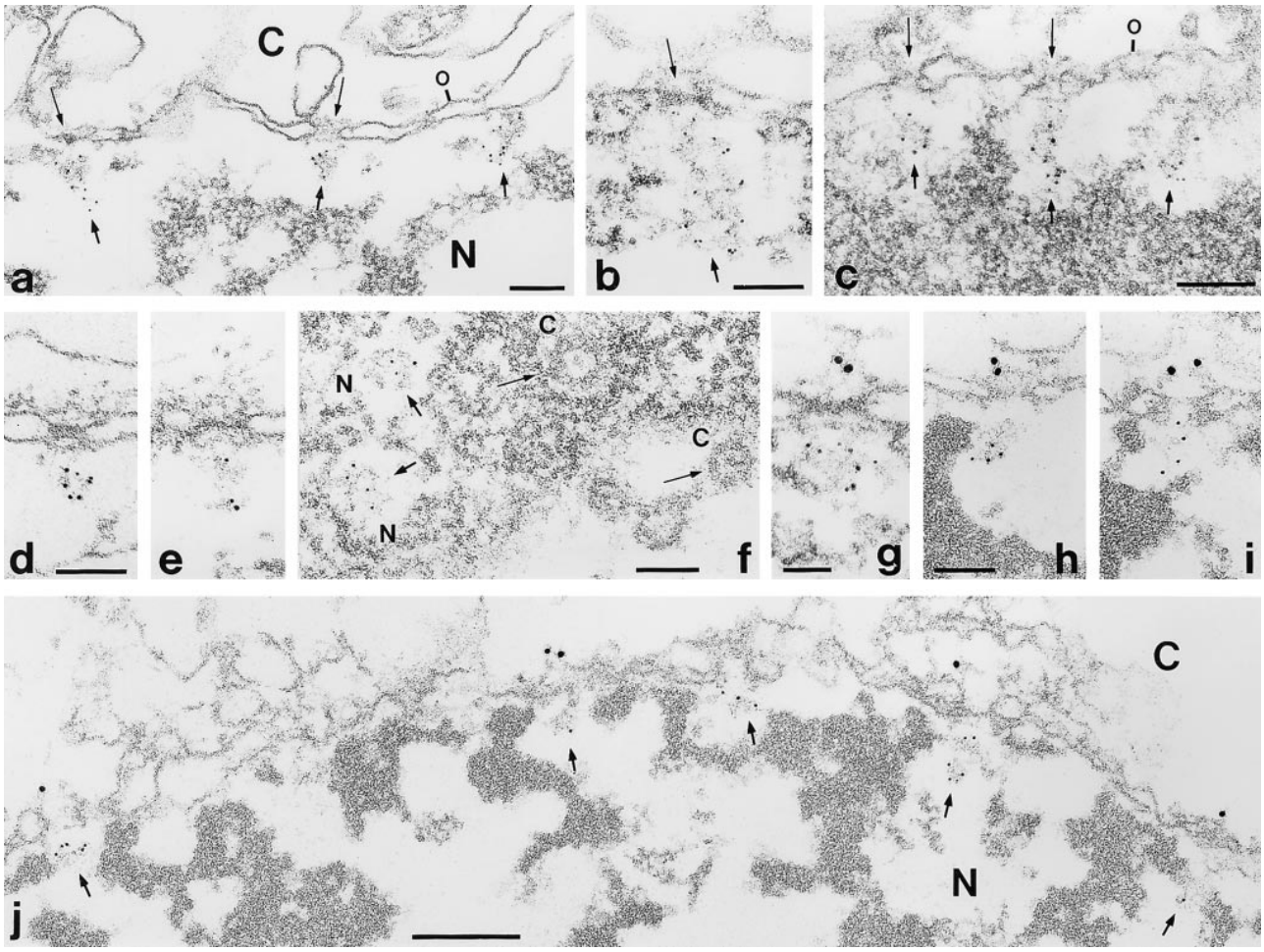

Figure 3. Immunoelectron microscopy of mammalian cells and tissues using mAb 203-37 in a preembedding technique, showing intense decoration of intranuclear sites near NPCs, often directly seen on the NPC-associated intranuclear filaments. Immunogold localization (5-nm gold–coupled secondary antibodies) of protein p270 on cryostat sections of human liver (*a–c*), bovine testis (*d* and *e*), and in detergent-permeabilized human PLC cells (*f*). Cross-sections presented in *a–e* reveal exclusive labeling at the nucleoplasmic side of the NPC and on the NPC-attached filaments extending into the nuclear interior. The grazing section presented in *f* allows insight into the nuclear interior (*N*), and reveals nucleoplasmic labeling of two NPCs or its associated filament bundles (*short thick arrows*) whereas no labeling is observed at the level of the outer, i.e., cytoplasmic annulus or in the mid-plane of the NPCs as demonstrable by the presence of a dense central granule (*long thin arrows*). (*g–j*) Double label immunogold EM on cryostat sections of human (*g*) and bovine (*h–j*) liver using mAb 203-37 (5-nm gold–coupled secondary antibodies) and affinity-purified guinea pig (*g*, gp-αRBP2-2) and rabbit antibodies (*h–j*, rb-αRBP2-2) against RanBP2/Nup358 (10-nm gold–coupled secondary antibodies); RanBP2 representing a marker protein for the cytoplasmic side of the NPC. Cryostat sections were fixed with acetone (*a*, *c*, and *h–j*) or formaldehyde (*b*, *d*, *e*, and *g*). PLC cells were fixed with formaldehyde and then permeabilized by digitonin treatment (*f*). *N*, nuclear interior. *C*, cytoplasmic side. The outer nuclear membrane (denoted *o* in some figures) is oriented to the top in *a–e* and *g–j*. Thin long arrows in some figures mark several NPCs at their cytoplasmic side; thicker and shorter arrows denote immunoreactive intranuclear filamentous material at or near NPCs. Bars: (*a–d*, *f–h*) 0.1 μm; same magnification in *d* and *e*, and in *h* and *i*; (*g*) 0.05 μm; (*j*) 0.2 μm.

cDNA Clones Encoding p270 Reveal Sequence Identity to Protein Tpr

Using mAb 203-37, we screened a human fetal brain expression library and isolated a total of six immunoreactive clones (T1–T6) that, on DNA sequencing, were recognized to encode protein Tpr (Fig. 4 *a*) recently localized exclusively to the cytoplasmic margin of NPCs (Byrd et al., 1994; Bangs et al., 1996). One cDNA clone, T1, contained the entire open reading frame, encoding a 2,363-aa polypeptide with a predicted molecular mass of 267,333 daltons. Sequence comparison between human fetal brain Tpr and the previously published, slightly shorter aa sequence (265,559 daltons) of human Tpr that had been deduced from various cDNAs isolated from fibroblast and fibrosarcoma cDNA libraries (Mitchell, 1992*a*,*b*; Byrd et al., 1994) showed three aa exchanges in the amino-terminal domain (positions 779, 906, and 1239) and an additional insertion of 14 mainly acidic aa in the carboxy-terminal domain of fetal brain Tpr (at position 1951) as the only differences between the two sequences (Fig. 4 *b*).

In vitro transcription–translation of cDNA clone T1 using the reticulocyte lysate system yielded a product of ~270 kD (Fig. 4 *c*) that was indistinguishable in mobility from p270 identified by immunoblotting of HeLa cell pro-

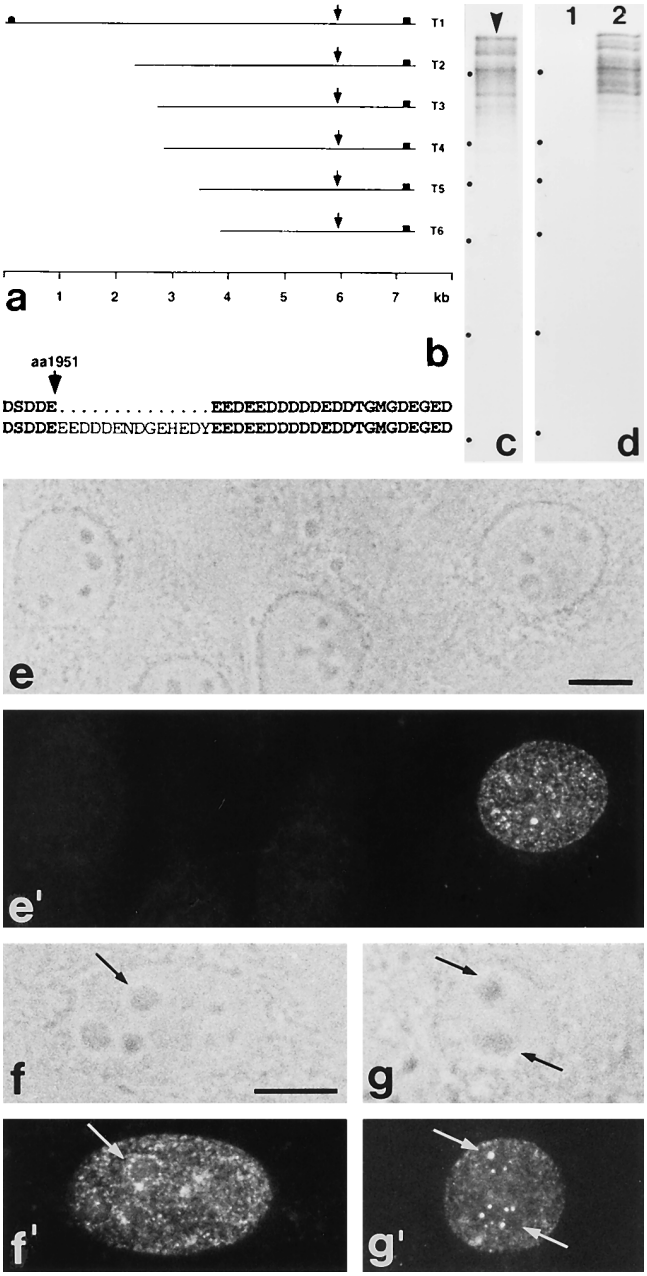

Figure 4. Characterization of p270 cDNA clones isolated from a human expression library using mAb 203-37. (*a*) Schematic presentation of human p270 cDNA clones isolated from a fetal brain Uni-Zap^{TM}XR cDNA library. Screening of this library with mAb 203-37 yielded one clone (T1: bp 1-7321) containing the entire coding region (bp 89-7177) for human Tpr, and five partial Tpr cDNA clones (T2: bp 2374-7321; T3: 2723-7321; T4: 2825-7321; T5: 3505-7321; T6: 3880-7321; lengths of polyA-tails varied between different clones and were omitted in the context of this bp numbering). The position of the AUG start codon in clone T1 is indicated by a circle, the stop codon present in all clones by squares. The ORF of T1 encodes a 2,363–residue protein with a predicted molecular mass of 267,333 D. Clones T3 and T4 represent fusion clones that also contain unrelated nt sequences at their 3′ end (not shown). Arrows denote the relative position of a sequence insertion, present in all clones, that occurs in addition to the previously published amino acid (aa) sequence of human Tpr and results in a prolonged acidic aa cluster (see *b*). The scale corresponds to the nt sequence of T1, each calibration line representing 1 kb. (*b*) An additional acidic aa sequence segment in human fetal brain Tpr. The top line shows the previously published aa sequence of human Tpr deduced from cDNA clones isolated from fibroblast and fibrosarcoma cDNA libraries (Mitchell and Cooper, 1992*a*,*b*). The bottom line shows the sequence of human fetal brain Tpr, containing 14 additional, mainly acidic aa. (*c*) Radiolabeled products obtained by in vitro transcription-translation of human Tpr cDNA clone T1 in reticulocyte lysate. The product with the lowest mobility (*arrowhead*) corresponds to a relative molecular mass of 270 kD. Radiolabeled polypeptides of lower relative masses may represent proteolytic products of Tpr or translation products resulting from misuse of sequence-internal AUG codons as translation initiation sites. Relative masses of reference proteins (positions denoted by dots on the left) are, from top to bottom, as follows: 205, 116, 97, 66, 45, and 29 kD. (*d*) Immunoprecipitation of radiolabeled human Tpr protein. In vitro translation products of cDNA clone T1 were incubated with protein G–Sepharose alone (lane *1*) or together with mAb 203-37 (lane *2*). Note that immunoabsorption of human Tpr from the reticulocyte lysate occurs only in the presence of mAb 203-37. Relative masses of reference proteins (dots on the left) are as in (*c*). (*e–g′*) Immunofluorescence microscopy on African green monkey kidney cells transfected with an expression vector encoding human fetal brain Tpr. Cells were stained with mAb 203-37 reactive with human Tpr, in transfected cells, but not with the endogenous monkey orthologue of Tpr. The same fields are shown in phase contrast (*e–g*) and epifluorescence optics (*e′–g′*). Besides a finely punctate nuclear labeling, reminiscent of NPC staining, intranuclear reaction sites are also noticeable. In a few transfected cells immunoreactive dots are located near the nucleoli (*arrows* in *f–g′*; compare also with Fig. 7, *f–g′*). Cells were fixed with methanol/acetone. Bars, 10 μm.

teins and was specifically immunoprecipitated by mAb 203-37 (Fig. 4 *d*), indicating that p270 and at least the human fetal brain variant of Tpr represent the same antigen.

Expression of the human fetal brain *tpr* gene under control of a CMV promoter in African green monkey cells (Fig. 4, *e–g′*) and in rodent cells of lines Faza-967-D2 and L-M(TK$^-$) (not shown) confirmed that this variant of the human Tpr protein is targeted to, and stably associates with, nuclear structures. Immunofluorescence microscopy on transfected cells using mAb 203-37 revealed both the finely punctate staining in the nuclear periphery reminiscent of NPC labeling and the occurrence of intranuclear speckles, which occasionally appeared close to the nucleoli (Fig. 4, *f–g′*). A similar nuclear localization of human fetal brain Tpr was also observed when an expression vector containing a major histocompatibility complex class I H-2 promoter was used (not shown). In some transfected cells, with a seemingly higher level of human Tpr protein synthesis, some punctate immunoreaction sites that remain to be characterized were also noticeable in the cytoplasm (not shown).

Antibodies against Different Epitopes of Protein Tpr React with p270

To exclude that mAb 203-37 immunoreacts only with a distinct Tpr variant located at the nucleoplasmic side of the NPC but not with the Tpr protein that had been localized to the cytoplasmic side of the NPC by Byrd et al. (1994), we raised antibodies against two peptides representing different regions of human Tpr that were identical

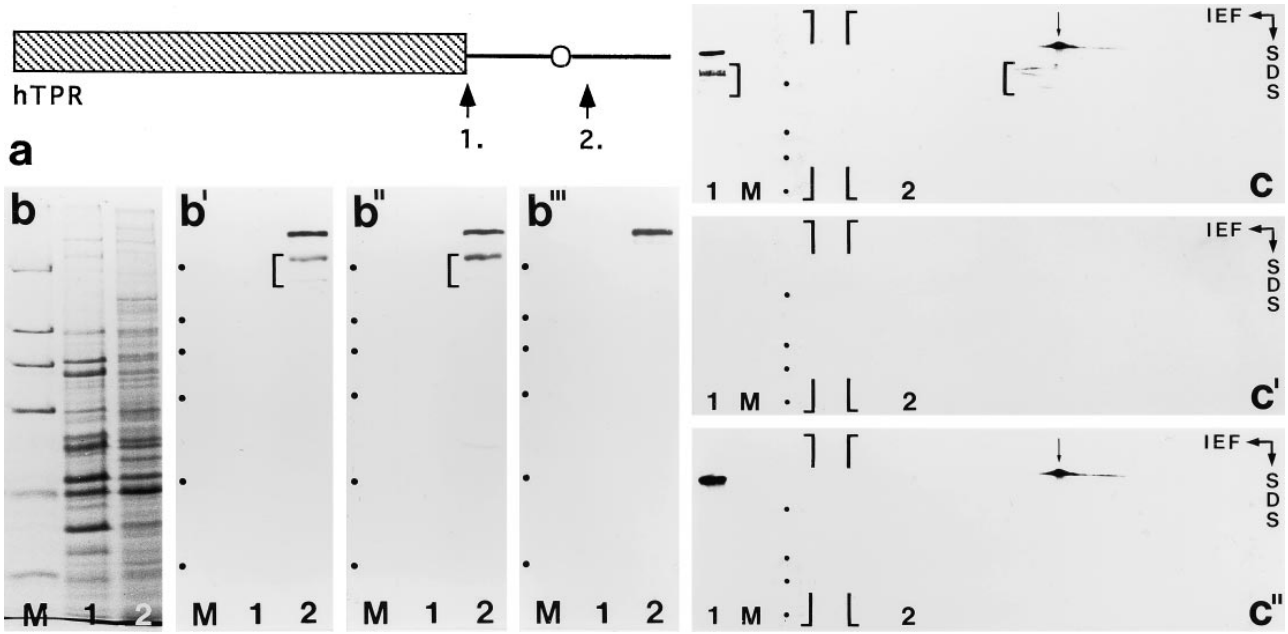

Figure 5. Immunoblot detection of p270 with affinity-purified guinea pig and rabbit antibodies raised against human Tpr protein. (*a*) Schematic presentation of human protein Tpr and the relative positions (*arrows*) of the two Tpr peptides, No. 1 (hTpr-Pep1, *1.*) and No. 2 (hTpr-Pep2, *2.*), against which antibodies were raised. The hatched box designates the amino-terminal domain of Tpr predicted to form α helices capable of forming coiled-coil structures. The carboxy-terminal domain (*black line*) is characterized by several acidic regions. The major cluster of acidic aa (corresponding to the cluster shown in Fig. 4 *b*) is designated by an open circle. Basic sequence elements (not denoted) separate the acidic regions and also characterize the ~50–carboxy-terminal aa. (*b–b‴*) SDS-PAGE of total HeLa cell proteins separated into a fraction of soluble proteins released by digitonin permeabilization of cells (lanes *1*) and of residual, nonextracted proteins (lanes *2*). Proteins were, in parallel, either stained by Coomassie blue (*b*) or transferred to nitrocellulose for immunodetection of proteins by ECL (*b′–b‴*). Same amounts of proteins were loaded in corresponding lanes of gels for Coomassie staining and immunoblotting. Digitonin treatment of HeLa cells already triggered proteolytic breakdown of protein Tpr and was applied to analyze immunoreaction of degradation products with different Tpr peptide antibodies. (*b′*) Immunoblot using mAb 203-37 as reference, showing the detection of protein p270/Tpr and a major putative degradation product of ~210-kD. (*b″*) Immunoblot using guinea pig antibodies against hTpr-Pep1 showing essentially the same result as obtained with mAb 203-37: besides predominant labeling of p270/Tpr, immunoreaction is also noticed with the ~210-kD polypeptide. (*b‴*) Immunoblot using rabbit antibodies against hTpr-Pep2 showing labeling of p270/Tpr whereas the shorter degradation product of ~210 kD is not immunoreactive. Note that hTpr-Pep2 is located nearer towards the protein's carboxy terminus than hTpr-Pep1. Relative masses of marker proteins (*M*) (denoted by dots in *b′-b‴*) are as in Fig. 2. (*c–c″*) Identification of p270 as protein Tpr by double immunoblotting with mAb 203-37 and rabbit antibodies raised against hTpr-Pep2. Residual HeLa proteins obtained after digitonin extraction were separated by IEF and SDS-PAGE and then transferred to a nitrocellulose filter (*2*). As reference, the same protein fraction was also separated on the left side of the same gel by SDS-PAGE alone (*1*), together with marker proteins (denoted by dots in lanes *M*) with relative masses, from top to bottom, of 205, 116, 97, and 66 kD. The filter (only the upper half is shown) was first incubated with mAb 203-37 and HRP-coupled secondary antibodies to murine Ig (*c*): the immunoblot reaction (ECL procedure, exposure time <1 min) identifies p270 (*arrow*) and putative degradation products (brackets in *1* and *2*) of ~210 kD. Bound antibodies were then released under acidic conditions and the filter incubated solely with HRP-coupled secondary antibodies to rabbit Ig (*c′*): ECL (exposure time >12 h) reveals no unspecific immunoreaction of p270 with these secondary antibodies. The filter then again was washed in acidic buffer and incubated with affinity-purified rabbit antibodies raised against hTpr-Pep2 (rb-αhTpr-Pep2) and HRP-coupled α-rabbit secondary antibodies: ECL (exposure time <1 min) shows specific labeling of protein Tpr (*arrow*). Note that proteins identified as p270 in *c* and as Tpr in *c″* are indistinguishable by electrophoresis. As expected, the 210-kD putative degradation product is not immunoreactive with rb-αhTpr-Pep2.

to both brain and fibroblast Tpr (Fig. 5 *a*). Immunoblotting using the affinity-purified antibodies revealed specific immunoreaction with p270 (Fig. 5, *b–b‴*). Moreover, both mAb 203-37 and the antibodies against human Tpr peptide no. 1 (Fig. 5 *a*) similarly reacted also with the same pattern of lower molecular weight polypeptides considered to represent p270 degradation products (Fig. 5, *b′* and *b″*). Two-dimensional gel electrophoresis followed by immunoblotting definitively proved that the same mAb 203-37 reactive protein p270 was indeed also detected with the Tpr peptide antibodies (Fig. 5, *c–c″*).

Antibodies against mammalian p270/Tpr either did not react with the *Xenopus laevis* Tpr orthologue or exhibited additional unspecific cross-reactions with other *Xenopus* proteins (not shown). We therefore also raised rabbit antibodies against the *Xenopus* Tpr protein. To this end, we first isolated a series of overlapping PCR products using a *Xenopus* kidney cDNA library as template and from which assembled a partial DNA sequence of 1,811 bp that encoded the 558 carboxy-terminal aa of the *Xenopus* Tpr protein (Fig. 6 *a*). This sequence exhibited a high degree of homology (70% identity) to the human sequence, including uninterrupted stretches of 27–45 identical aa. For immunization, a peptide located near the carboxy terminus (Fig. 6 *b*) was chosen, yielding antibodies that specifically reacted with the *Xenopus* p270/Tpr protein on total pro-

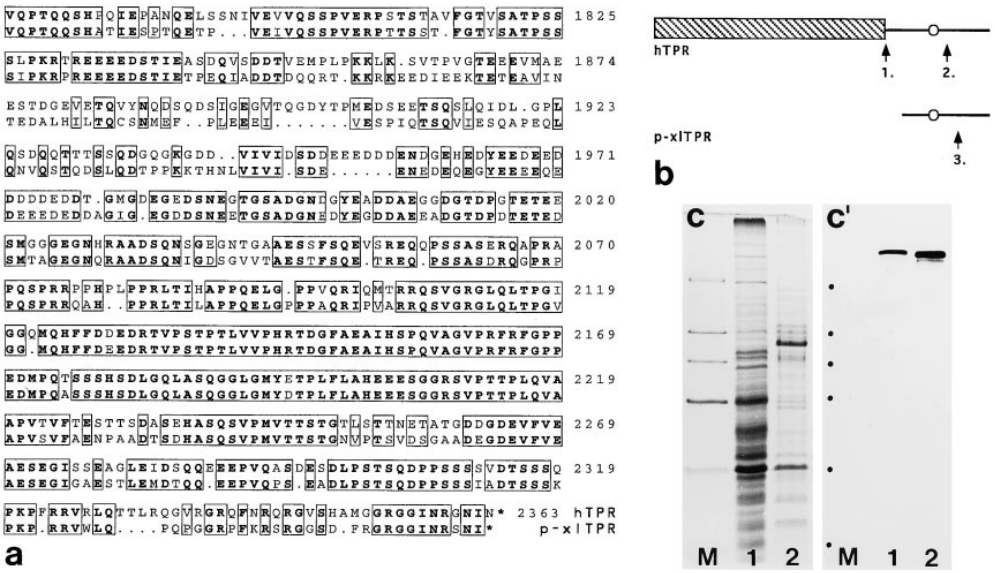

Figure 6. Generation of antibodies immunoreactive with amphibian Tpr. (*a*) Isolation of PCR products encoding the carboxy-terminal domain of the *Xenopus laevis* Tpr protein and alignment of human and *Xenopus* Tpr aa sequences. A *Xenopus* kidney cDNA library was used as template for PCR assays. Several overlapping DNA fragments were assembled into a partial DNA sequence of 1811 bp that encodes the 558–carboxy-terminal aa of *Xenopus* Tpr (p-xlTPR) shown in the bottom lane of the alignment; the corresponding human sequence is shown in the upper lane (hTPR). Numbers at the right margin stand for aa positions in accordance to full-length human fetal brain Tpr. Identical aa (*bold letters*) and homologous aa are boxed. Groups of homologous aa as relevant for this alignment were laid down as follows: R+K; D+E; S+T; V+A+P; V+I+L+M. (*b*) Schematic presentation of the partial *Xenopus* Tpr aa sequence (p-xlTPR) and the relative position (*arrow*) of a *Xenopus* Tpr peptide, xlTpr-Pep3 (*3.*), against which antibodies were raised. The human Tpr scheme (hTPR) with its relative peptide positions is shown as a reference. (*c*) Immunodetection of *Xenopus* protein p270/Tpr with affinity-purified rabbit antibodies raised against xlTpr-Pep3. Total proteins from *Xenopus laevis* kidney epithelial cells (lanes *1*) and from manually isolated *Xenopus* oocyte nuclei (lanes *2*) were separated by SDS-PAGE and, in parallel, either stained by Coomassie blue (*c*) or transferred to nitrocellulose for immunodetection of proteins by ECL (*c′*). Same amounts of protein were loaded in corresponding lanes of *c* and *c′*. Relative masses of marker proteins (*M*) in *c* (denoted by dots in *c′*) are as in Fig. 2.

teins of *Xenopus* kidney epithelial cells of line A6 and of manually isolated oocyte nuclei (Fig. 6, *c* and *c′*).

Antibodies against Human and Xenopus p270/Tpr Label NPC-attached Intranuclear Filaments

Immunofluorescence microscopy using the human p270/Tpr peptide antibodies on cultured mammalian cells and on cryostat sections of mammalian tissues (liver, esophagus, epidermis, and colon) yielded results (some are shown in Fig. 7, *a–d*) that were essentially indistinguishable from those obtained with mAb 203-37 (compare with Fig. 1) but revealed broader cross-reactivity between the various mammalian species, including rodents and African green monkey cells (not shown). The antibodies against the *Xenopus* p270/Tpr sequence equally resulted in punctate staining of the nuclear periphery of cultured *Xenopus* cells with some occasional intranuclear speckles (Fig. 7, *e–g′*). Punctate nuclear periphery staining was further noticed in *Xenopus* erythrocytes (not shown). On cryostat sections of *Xenopus* skin, liver, and oocytes (Fig. 7, *h* and *h′*), immunolabeling was seen at the nuclear envelope and occasionally, in somatic cells, also in additional intranuclear dots (not shown).

In contrast with several other NPC proteins, p270/Tpr was not detected in the pore complex–containing cytoplasmic annulate lamellae as revealed by double immunofluorescence microscopy on different mammalian and amphibian cells (Fig. 8), using the above described antibodies against p270/Tpr and such against NPC proteins that have been demonstrated to represent marker molecules for annulate lamellae (Cordes et al., 1995, 1996).

Immunoelectron microscopy using preembedding immunogold labeling (secondary antibodies coupled to 5-nm colloidal gold) revealed identical results on human liver sections with antibodies against human Tpr peptides Nos. 1 and 2. Both antibodies specifically labeled the NPC-attached intranuclear filaments, whereas the cytoplasmic side of the NPC was devoid of gold particles (Fig. 9, *a–d*). Essentially identical results were obtained on cryostat sections of human epidermis (not shown). As already noticed by immunoelectron microscopy using mAb 203-37 (see above), we occasionally also noticed specific immunolabeling of yet unidentified small intranuclear spheroidal structures (Fig. 9 *e*). To control for the accessibility of both sides of the NPC, double immunogold label localizations with antibodies against RanBP2/Nup358 (10-nm gold–coupled secondary antibodies) and p270/Tpr (5-nm gold) were performed. The larger RanBP2 immunogold particles were seen almost exclusively at the outer NPC annulus (Fig. 9, *f–h*), thus confirming the localizations of others (Wu et al., 1995; Yokoyama et al., 1995; Wilken et al., 1995). This differential double label therefore underscores the significance of the intranuclear location of protein p270/Tpr.

Immunogold labeling on manually isolated stage VI oocytes of *Xenopus laevis*, using rabbit antibodies against peptide No. 3 of the *Xenopus* p270/Tpr protein and secondary antibodies coupled to 5-nm gold particles (Fig. 10, *a–d*), resulted in a very dense and specific decoration of the NPC-attached intranuclear filament bundles, whereas both the outer aspect of the NPC and the pore complexes of annulate lamellae were free of immunogold label. In some micrographs with structurally well-preserved filament bundles, the gold-decorated filaments projected into

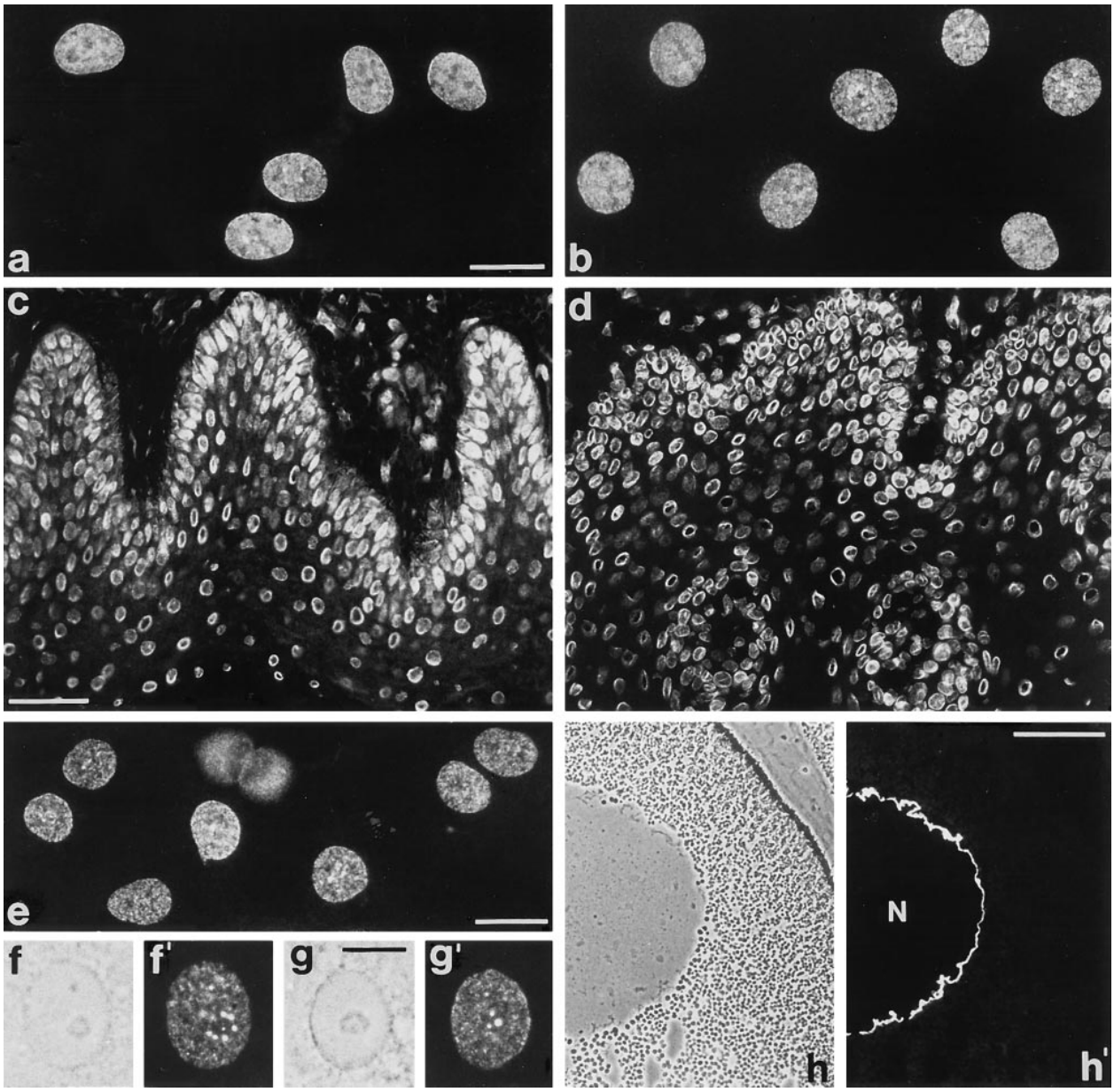

Figure 7. Immunofluorescence microscopy of cultured cells and tissue cryostat sections after reaction with affinity-purified guinea pig and rabbit antibodies raised against different epitopes of human and *Xenopus* Tpr. (*a*) HeLa cells stained with guinea pig antibodies against hTpr-Pep1 (gp-αhTpr-Pep1). (*b*) Bovine mammary gland epithelial cells of line BMGE stained with rabbit antibodies against hTpr-Pep2 (rb-αhTpr-Pep2). (*c* and *d*) Cryostat section of human epidermis (*c*) stained with gp-αhTpr-Pep1 and human esophagus (*d*) stained with rb-αhTpr-Pep2. Note that the nuclear staining obtained with these antibodies is essentially indistinguishable from that obtained with mAb 203-37 (see Fig. 1). In addition to the finely punctate nuclear staining resembling immunolabeling of NPCs, immunoreactive intranuclear dots are also observed occasionally (*a* and *b*). (*e–g′*) *Xenopus laevis* kidney epithelial cells stained with rabbit antibodies against xlTpr-Pep3 (rb-αxlTpr-Pep3). In addition to the finely punctate nuclear labeling, intranuclear dots are noticed in a minor proportion of cells in which they sometimes appear to surround the nucleoli (*f–g′*). (*h* and *h′*) Cryostat sections through a *Xenopus* oocyte stained with rb-αxlTpr-Pep3. Epifluorescence (*a–e*; *f′*, *g′*, and *h′*) and corresponding phase contrast optics (*f*, *g*, and *h*) are shown. Cultured cells were fixed with methanol/acetone (*a*, *e–g′*) or formaldehyde followed by detergent treatment (*b*). Cryostat sections were fixed with formaldehyde (*c*) or acetone (*d* and *h*). *N*, nucleus. Bars: (*a* and *e*) 20 μm; same magnification in *b*; (*c*) 50 μm; same magnification in *d*; (*g*) 10 μm; same magnification in *f*; (*h′*) 100 μm.

the nuclear interior for up to 350 nm. Double label immunogold localization performed as control on manually isolated oocytes (Fig. 10, *e–j*) and on cryostat sections through *Xenopus* ovaries (Fig. 10 *k*), using antibodies against RanBP2/Nup358 (10-nm gold) and p270/Tpr (5-nm gold), showed the localization of RanBP2 at both the cytoplasmic margin of the NPCs and the cytoplasmic pore complexes of annulate lamellae (Fig. 10 *j*; see also Cordes et al., 1996), whereas the p270/Tpr protein again was localized to the intranuclear filaments.

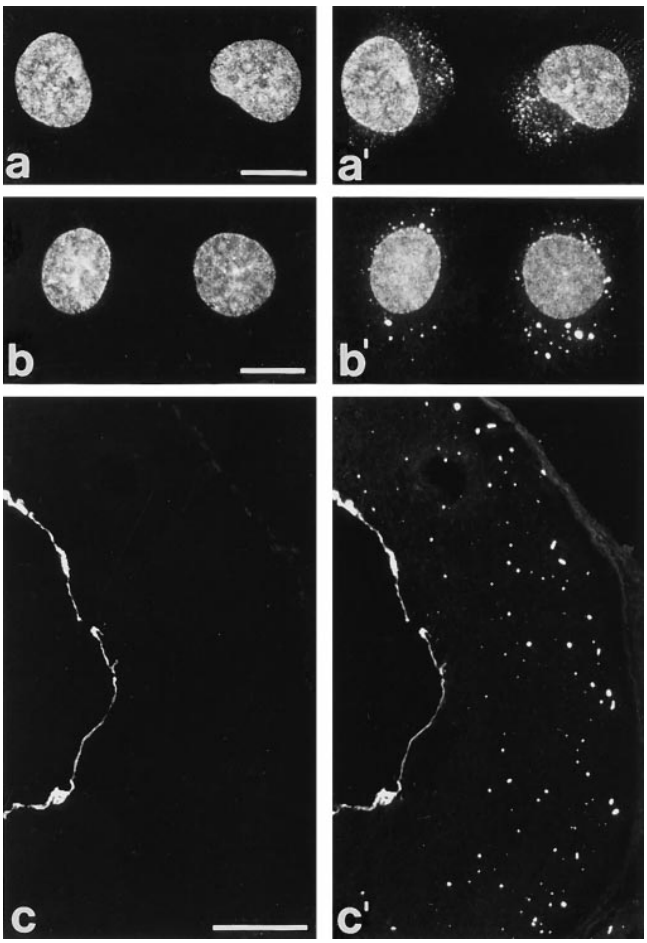

Figure 8. Double immunofluorescence microscopy of mammalian and amphibian cells using antibodies against p270/Tpr (*a–c*), and against other NPC proteins (*a′–c′*) that represent marker proteins for pore complexes both of the nuclear envelope and the cytoplasmic annulate lamellae. (*a* and *a′*) HeLa cells immunolabeled with mAb 203-37 against human Tpr (*a*) and affinity-purified guinea pig antibodies (gp-αRBP2-2) against RanBP2/Nup358 (*a′*). (*b* and *b′*) Bovine mammary gland epithelial cells of line BMGE immunolabeled with (*b*) affinity-purified rabbit antibodies against hTpr-Pep2 (rb-αhTpr-Pep2) and (*b′*) mAb 414 reactive with the XFXFG-family of O-glycosylated nucleoporins. (*c* and *c′*) Cryostat section through a *Xenopus laevis* stage VI oocyte immunolabeled with (*c*) affinity-purified rabbit antibodies against xlTpr-Pep3 (rb-αxlTpr-Pep3) and (*c′*) gp-αRBP2-2. Note that no cytoplasmic staining is detectable with Tpr-antibodies whereas distinctive cytoplasmic structures, representing annulate lamellae, are immunoreactive with antibodies against other NPC proteins. Secondary antibodies were coupled to cyanine 2-OSu bisfunctional (*a* and *c′*) or fluorescein isothiocyanate (*b′*) and cyanine 3.29-OSu (*a′* and *c*) or Texas red sulfonyl chloride (*b*). Cultured cells were fixed with methanol/acetone (*a* and *a′*) or formaldehyde followed by detergent treatment (*b* and *b′*). The oocyte cryostat section was fixed with acetone (*c* and *c′*). Bars: (*a* and *b*) 15 μm; (*c*) 100 μm.

Discussion

We have identified a ~270-kD protein (p270) as a novel and constitutive component of the NPC-attached intranuclear filaments in diverse kinds of mammalian and amphibian cells. Analysis of cDNAs encoding human p270 and immunobiochemistry have then revealed that p270 corresponds to the previously described human Tpr protein (Mitchell and Cooper, 1992*a*,*b*), which, however, has been reported to be exclusively located on the cytoplasmic side of the NPC (Byrd et al., 1994; Bangs et al., 1996; for review see Pante and Aebi 1995*a*,*b*, 1996; Bastos et al., 1995; Goldberg and Allen, 1995). Because of this discrepancy and because the sequence of 2,363 aa in our p270 cDNA isolated from human fetal brain contained several additional aa and a few minor changes compared with the aa sequence (2,349 aa) assembled from different partial human fibroblast and fibrosarcoma cDNAs (Mitchell and Cooper, 1992*a*,*b*; Byrd et al., 1994), we took special care to prove the identity of p270 and Tpr by raising antibodies against peptides representing different epitopes common to both human Tpr aa sequences. All antibodies obtained specifically react with the same p270 polypeptide and immunolabel the same NPC-attached intranuclear filaments that are also positive with the mAb against p270 initially used. By contrast, the cytoplasmic annulus of the NPC has been devoid of immunolabel although it is perfectly accessible, as confirmed by double immunoelectron microscopy using RanBP2/Nup358, a bona fide marker of the cytoplasmic NPC aspect (Yokoyama et al., 1995; Wu et al., 1995; Wilken et al., 1995) as control antigen. These immunolocalization results are also consistent with our observations made in digitonin-permeabilized cells, following the procedure recently used by others to prove exclusively cytoplasmic side labeling of NPCs (Bangs et al., 1996). We noticed that under these conditions only some of the nuclei were immunolabeled with p270/Tpr antibodies, whereas others were totally negative, indicating that the antigen was not accessible. Using RanBP2 antibodies, all nuclei, in contrast, were immunolabeled.

The amphibian oocyte (germinal vesicle) represents a particularly suitable "classic" system to study structural aspects of the NPC and its attached filaments. Therefore, we have isolated PCR products encoding the *Xenopus* p270/Tpr protein, raised antibodies to it, and performed immunoelectron microscopy on mature oocytes of *Xenopus laevis.* The results have essentially confirmed those obtained with mammalian cells: immunogold decorates intensely and specifically the NPC-attached intranuclear filament bundles, whereas the cytoplasmic side of the NPC does not react. In these cells, the NPC-attached intranuclear bundles are particularly well developed (see also Franke and Scheer, 1970*a*,*b*, 1974; Richardson et al., 1988; Cordes et al., 1993; Ris and Malecki, 1993) and project into the nuclear interior, clearly exceeding the ~50 nm of the NPC-attached intranuclear fish trap or basket structures (Ris, 1989, 1991; Jarnik and Aebi, 1991; Goldberg and Allen, 1992). It is also obvious from our study that these filament bundles projecting from a given NPC into the nucleoplasm represent a distinct structural entity, in agreement with the observations of Ris and Malecki (1993) with glutaraldehyde-fixed cylindrical bundles of NPC-attached filaments (see, e.g., Fig. 3, *b* and *c*, in Ris and Malecki, 1993). Our tracings of p270/Tpr-containing filament bundles for up to 200 nm in mammalian somatic cells and for up to 350 nm in *Xenopus* oocytes and the absence of label on the interporous aspects of the nuclear envelope further indicate that these filamentous structures are not systematic artifacts originated

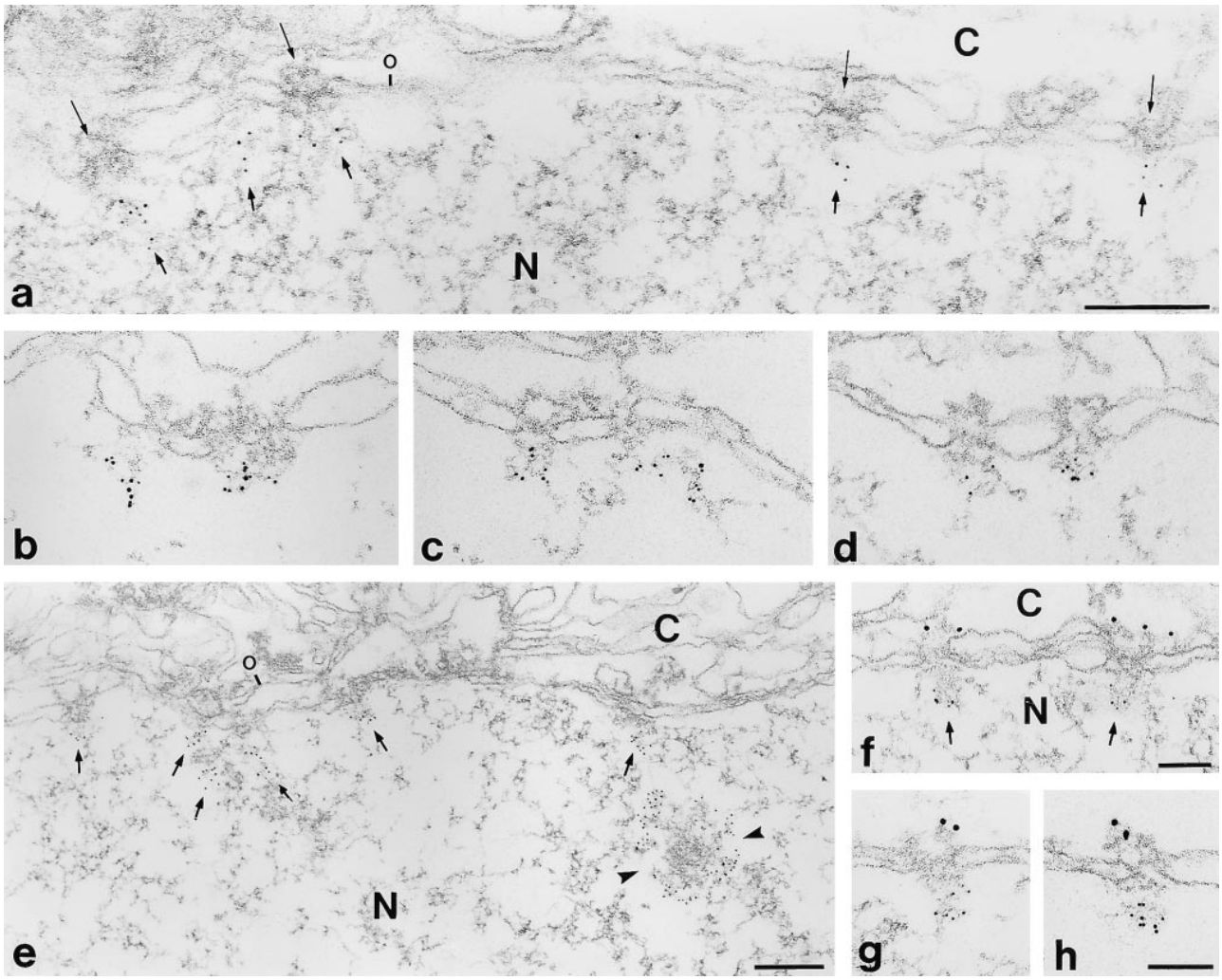

Figure 9. Immunoelectron microscopy of human tissues after reaction with affinity-purified antibodies raised against different epitopes of human Tpr revealing exclusive intranuclear localization of protein p270/Tpr. (*a–e*) Immunogold localization (5-nm-gold) of p270/Tpr on cryostat sections of human liver using rabbit antibodies (rb-αhTpr-Pep2) against hTpr-Pep2 (*a–c*, and *e*) and guinea pig antibodies (gp-αhTpr-Pep1) against hTpr-Pep1 (*d*). Thin long arrows in some figures mark several NPCs at their cytoplasmic side; thicker and shorter arrows denote immunoreactive intranuclear filaments. In addition to the immunolocalization of p270/Tpr in NPC-attached filamentous material, labelings of electron-dense spheroidal intranuclear structures (*arrowheads* in *e*) are occasionally observed. (*f–h*) Double label immunogold EM on cryostat sections of human liver confirming the exclusively intranuclear localization of protein p270/Tpr. (*f* and *g*) rb-αhTpr-Pep2 (5-nm-gold) and guinea pig antibodies (gp-αRBP2-2) against RanBP2/Nup358 (10-nm-gold). (*h*) gp-αhTpr-Pep1 (5-nm-gold) and rabbit antibodies (rb-αRBP2-2) against RanBP2/Nup358 (10-nm-gold). Cryostat sections were fixed with acetone (*a–g*) or formaldehyde (*h*). *N*, nuclear interior. *C*, cytoplasmic side. The outer nuclear membrane (denoted *o* in some figures) is oriented to the top in all figures. Bars: (*a–e*) 0.2 μm, same magnification in *a–d*; (*f–h*) 0.1 μm; same magnification in *g* and *h*.

from ruptures of the nuclear envelope–subjacent filament lattice (Goldberg and Allen, 1992, 1995).

In addition to the immunoreactive NPC-attached filaments, we have also noticed, in a minor proportion of cells, immunolabeling of unknown small spheroidal intranuclear structures that sometimes surround nucleoli. Antibodies reactive with other spheroidal intranuclear marker structures all have been negative on these "Tpr-positive speckles" (data not shown), so that these structures could not be related to any of the known kinds of "nuclear bodies" (for examples and references see, e.g., Bohmann et al., 1995; Roth, 1995; Gall et al., 1995). Experiments to correlate the appearance of these structures with a specific cell cycle phase have also been inconclusive, as cell populations synchronized by colcemid or thymidine blocking and released into G1 or G2 did not contain significantly higher numbers of such intranuclear speckles (data not shown). At the moment, we cannot exclude that these immunoreactive dots merely represent accidental intranuclear aggregates of protein p270/Tpr.

From the intense decoration of mammalian and amphibian NPC-attached intranuclear filaments with antibodies against near carboxy-terminal epitopes of protein p270/Tpr, we conclude that in situ, i.e., in the actual filaments, all these epitopes are exposed and readily accessible, and thus probably located on the outer aspect of the filamentous cylinders. Sequence comparison between human and amphibian p270/Tpr shows that the carboxy-ter-

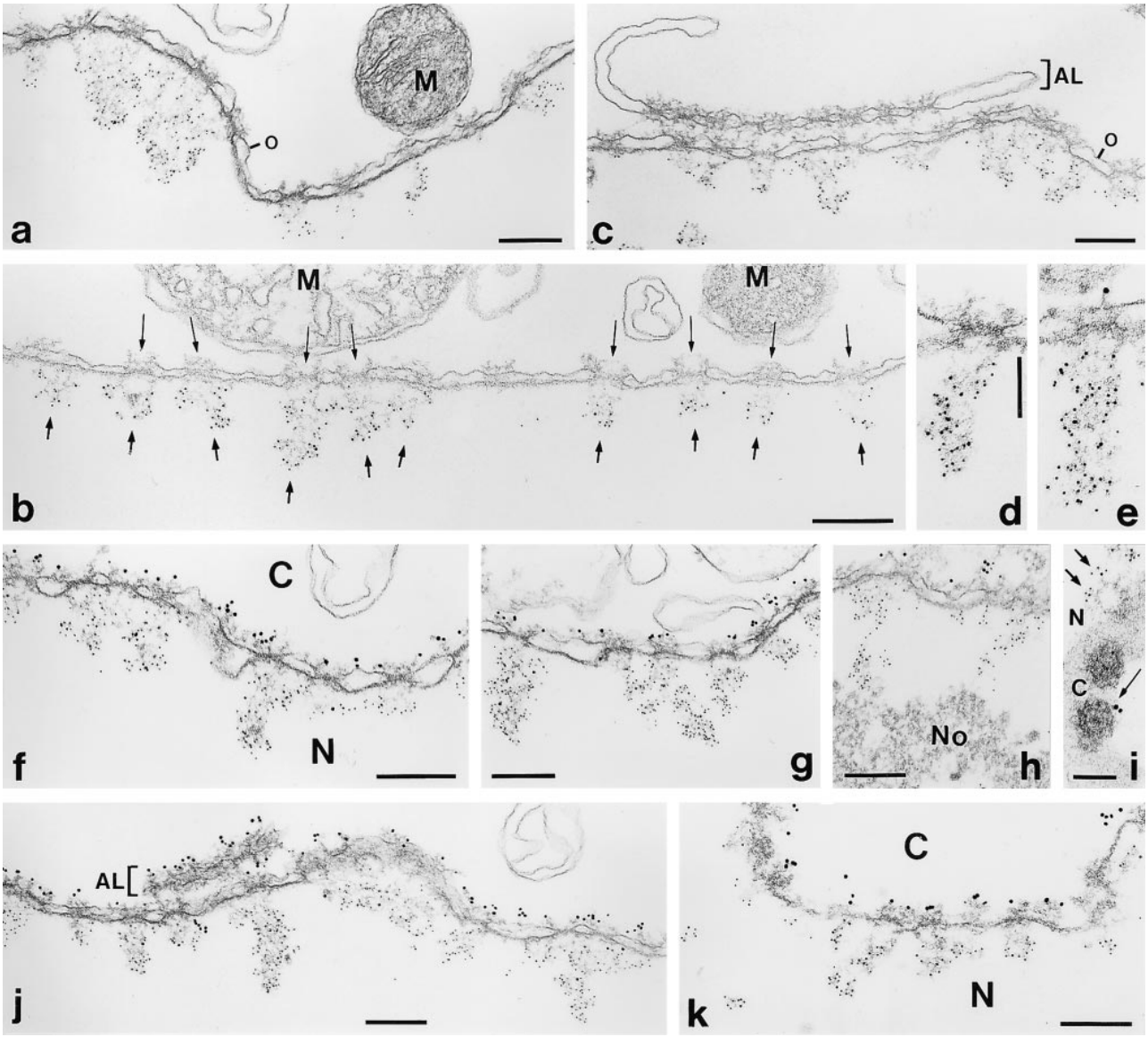

Figure 10. Immunoelectron microscopy of *Xenopus* oocytes after reaction with affinity-purified antibodies raised against *Xenopus* p270/Tpr showing dense labeling of NPC-attached intranuclear filament bundles. (*a–d*) Immunogold localization (5-nm-gold) of *Xenopus* p270/Tpr on manually isolated nuclei using rabbit antibodies raised against xlTpr-Pep3 (rb-αxlTpr-Pep3). Note the exclusive localization of p270/Tpr in the intranuclear NPC-attached filament bundles that often appear laterally aggregated and partly entangled. An individual, nuclear envelope-attached annulate lamellae cisterna (*AL*, marked by a bracket in *c*) is devoid of gold grains. (*e–k*) Double label immunogold EM on manually isolated nuclei (*e–j*) and on a formaldehyde-fixed cryostat section through an oocyte (*k*) using rb-αxlTpr-Pep3 (5-nm-gold) and guinea pig antibodies (gp-αRBP2-2) against RanBP2/Nup358 (10-nm-gold). Note that RanBP2 antibodies almost exclusively label the cytoplasmic side of the NPCs, whereas Tpr antibodies label intranuclear filaments. The grazing section through part of the nuclear envelope presented in *i* also shows the location of RanBP2 at the cytoplasmic side (*C*) of an NPC (*long thin arrow*), and Tpr at its nucleoplasmic (*N*) side. Note that protuberances extending from the corners of the NPCs eightfold symmetrical inner cylinder or annulus are labeled by Tpr antibodies (*short thick arrows*). Also, in *h*, intranuclear filaments extend far into the nuclear interior and occasionally interconnect nucleoli (*No*) and NPCs. Also note, in *j*, that cytoplasmic pore complexes of annulate lamellae, immunonegative for Tpr, are labeled by RanBP2 antibodies. Numbers of occasionally observed intranuclear 10-nm-gold grains and cytoplasmic 5-nm-gold were in the range of unspecific background labeling and secondary antibody cross-reactivities. The outer nuclear membrane (*o*) is oriented to the top in *a–h* and *j–k.* Thin long arrows in *b* mark several NPCs at their cytoplasmic side; thick short arrows denote intranuclear sites of Tpr labeling. *M*, mitochondria. Bars: (*a–c*, *f–h*, *j*, and *k*) 0.2 μm; (*d* and *i*) 0.1 μm, same magnification in *d* and *e.*

minal domain is highly conserved and rich in acidic aa, and therefore a reasonable candidate for interactions with basic proteins known to occur in chromatin as well as in ribonucleoprotein particles. Experiments to identify complexes of p270/Tpr with other nuclear proteins and to examine its possible involvement in filament-guided nucleocytoplasmic transport processes (see also the "tracks" of Blobel, 1985; Meier and Blobel, 1992; Stroboulis and Wolffe, 1996)

are currently underway in our laboratory. The conspicuously long and dense NPC-attached filament bundles in amphibian oocytes might further indicate that in these particular cells, p270/Tpr and the filaments containing it belong to those elements that are also maternally stored to serve important roles in early embryogenesis.

The amino-terminal domain of the p270/Tpr protein contains numerous leucine zipper motifs and regions of heptad repeats typical of α helices organized in coiled-coils (Mitchell and Cooper, 1992*b*). Such a predicted conformation makes this protein a very likely candidate for assemblies of stable homo- or heterodimers (see also Byrd et al., 1994) and for participation in the formation of the backbone of the intranuclear filaments described. This hypothesis should now be directly testable by self-assembly experiments in vitro, using the pure protein made by recombinant technology.

We thank Andreas Hunziker for competent help in DNA sequencing, Horst Baron for technical assistance in immunizing animals, and Jutta Müller-Osterholt for photography. We also thank Rudi Zirwes for providing the *Xenopus laevis* cDNA library and Drs. Harald Herrmann, Karsten Weis, Ralf Bischoff, and Georg Krohne for valuable discussions.

The human fetal brain p270/Tpr sequence and the partial *Xenopus* kidney sequence have been submitted to the GenBank and are available under accession numbers U69668 and U69669, respectively.

Received for publication 30 September 1996 and in revised form 27 November 1996.

References

Akey, C.W., and M. Rademacher. 1993. Architecture of the *Xenopus* nuclear pore complex revealed by three-dimensional cryo-electron microscopy. *J. Cell Biol.* 122:1–20.

Bangs, P.L., C.A. Sparks, P.R. Odgren, and E.G. Fey. 1996. Product of the oncogene-activating gene *Tpr* is a phosphorylated protein of the nuclear pore complex. *J. Cell. Biochem.* 61:48–60.

Bastos, R., N. Pante, and B. Burke. 1995. Nuclear pore complex proteins. *Int. Rev. Cytol.* 162B:257–302.

Blobel, G. 1985. Gene gating: a hypothesis. *Proc. Natl. Acad. Sci. USA*. 82: 8527–8529.

Bohmann, K., J. Ferreira, N. Santama, K. Weis, and A.I. Lamond. 1995. Molecular analysis of the coiled body. *J. Cell Sci. Suppl.* 19:107–113.

Byrd, D.A., D.J. Sweet, N. Pante, K.N. Konstantinov, T. Guan, A.C.S. Saphire, P.J. Mitchell, C.S. Cooper, U. Aebi, and L. Gerace. 1994. Tpr, a large coiled coil protein whose amino terminus is involved in activation of oncogenic kinases, is localized to the cytoplasmic surface of the nuclear pore complex. *J. Cell Biol.* 127:1515–1526.

Chardonnet, Y., and S. Dales. 1972. Early events in the interaction of Adenovirus with HeLa cells. III. Relationship between an ATPase activity in nuclear envelopes and transfer of core material: a hypothesis. *Virology.* 48:342–350.

Cordes, V.C., S. Reidenbach, A. Köhler, N. Stuurman, R. van Driel, and W.W. Franke. 1993. Intranuclear filaments containing a nuclear pore complex protein. *J. Cell Biol.* 123:1333–1344.

Cordes, V.C., S. Reidenbach, and W.W. Franke. 1995. High content of a nuclear pore protein in cytoplasmic annulate lamellae of *Xenopus* oocytes. *Eur. J. Cell Biol.* 68:240–255.

Cordes, V.C., S. Reidenbach, and W.W. Franke. 1996. Cytoplasmic annulate lamellae in cultured cells: composition, distribution, and mitotic behavior. *Cell Tissue Res.* 283:177–191.

Davis, L.I. 1995. The nuclear pore complex. *Annu. Rev. Biochem.* 64:865–896.

Davis, L.I., and G. Blobel. 1986. Identification and characterization of a nuclear pore complex protein. *Cell.* 45:699–709.

Emini, E.A., J.V. Hughes, D.S. Perlow, and J. Boger. 1985. Induction of hepatitis A virus-neutralizing antibody by a virus-specific peptide. *J. Virol.* 55:836–839.

Feldherr, C.M. 1974. The binding characteristics of the nuclear annuli. *Exp. Cell Res.* 85:271–277.

Franke, W.W. 1966. Isolated nuclear membranes. *J. Cell Biol.* 31:619–623.

Franke, W.W. 1970. On the universality of nuclear pore complex structure. *Z. Zellforsch.* 105:405–429.

Franke, W.W. 1974. Structure, biochemistry, and functions of the nuclear envelope. *Int. Rev. Cytol.* 4:72–237.

Franke, W.W., and U. Scheer. 1970*a.* The ultrastructure of the nuclear envelope of amphibian oocytes: a reinvestigation. I. The mature oocyte. *J. Ultrastruct. Res.* 30:288–316.

Franke, W.W., and U. Scheer. 1970*b.* The ultrastructure of the nuclear envelope of amphibian oocytes: a reinvestigation. II. The immature oocyte and dynamic aspects. *J. Ultrastruct. Res.* 30:317–327.

Gall, J.G. 1967. Octagonal nuclear pores. *J. Cell Biol.* 32:391–399.

Gall, J.G., A. Tsvetkov, Z. Wu, and C. Murphy. 1995. Is the sphere organelle/coiled body a universal nuclear component? *Dev. Genet.* 16:25–35.

Gerace, L., Y. Ottaviano, and C. Kondor-Koch. 1982. Identification of a major polypeptide of the nuclear pore complex. *J. Cell Biol.* 95:826–837.

Goldberg, M.W., and T.D. Allen. 1992. High resolution scanning electron microscopy of the nuclear envelope: demonstration of a new, regular, fibrous lattice attached to the baskets of the nucleoplasmic face of the nuclear pores. *J. Cell Biol.* 119:1429–1440.

Goldberg, M.W., and T.D. Allen. 1995. Structural and functional organization of the nuclear envelope. *Curr. Opin. Cell Biol.* 7:301–309.

Greco, A., M.A. Pierotti, I. Bongarzone, S. Pagliardini, C. Lanzi, and G. Della Porta. 1992. TRK-T1 is a novel oncogene formed by the fusion of TPR and TRK genes in human papillary thyroid carcinomas. *Oncogene.* 7:237–242.

Hallberg, E., R.W. Wozniak, and G. Blobel. 1993. An integral membrane protein of the pore membrane domain of the nuclear envelope contains a nucleoporin-like region. *J. Cell Biol.* 122:513–521.

Hinshaw, J.E., B.O. Carragher, and R.A. Milligan. 1992. Architecture and design of the nuclear pore complex. *Cell.* 69:1133–1141.

Höger, T.H., C. Grund, W.W. Franke, and G. Krohne. 1991. Immunolocalization of lamins in the thick nuclear lamina of human synovial cells. *Eur. J. Cell Biol.* 54:150–156.

Jarnik, M., and U. Aebi. 1991. Towards a more complete 3-D structure of the nuclear pore complex. *J. Struct. Biol.* 107:291–308.

Jameson, B.A., and H. Wolf. 1988. The antigenic index: a novel algorithm for predicting antigenic determinants. *Comput. Appl. Biosci.* 4:181–186.

Kartenbeck, J., H. Zentgraf, U. Scheer, and W.W. Franke. 1971. The nuclear envelope in freeze-etching. *Adv. Anat. Embryol. Cell Biol.* 45:1–55.

Kraemer, D., R.W. Wozniak, G. Blobel, and A. Radu. 1994. The human CAN protein, a putative oncogene product associated with myeloid leukemogenesis, is a nuclear pore complex protein that faces the cytoplasm. *Proc. Natl. Acad. Sci. USA.* 91:1519–1523.

Laemmli, U.K. 1970. Cleavage of structural proteins during the assembly of the head of bacteriophage T4. *Nature (Lond.).* 227:680–685.

Leube, R.E., U. Leimer, C. Grund, W.W. Franke, N. Harth, and B. Wiedenmann. 1994. Sorting of synaptophysin into special vesicles in nonneuroendocrine epithelial cells. *J. Cell Biol.* 127:1589–1601.

Meier, U.T., and G. Blobel. 1992. Nopp140 shuttles on tracks between nucleolus and cytoplasm. *Cell.* 70:127–138.

Melchior, F., and L. Gerace. 1995. Mechanism of nuclear protein import. *Curr. Opin. Cell Biol.* 7:310–318.

Melchior, F., T. Guan, N. Yokoyama, T. Nishimoto, and L. Gerace. 1995. GTP hydrolysis by Ran occurs at the nuclear pore complex in an early step of protein import. *J. Cell Biol.* 131:571–581.

Mitchell, P.J., and C.S. Cooper. 1992*a.* Nucleotide sequence analysis of human *tpr* cDNA clones. *Oncogene.* 7:383–388.

Mitchell, P.J., and C.S. Cooper. 1992*b.* The human tpr gene encodes a protein of 2094 amino acids that has extensive coiled-coil regions and an acidic C-terminal domain. *Oncogene.* 7:2329–2333.

Newmeyer, D.D., and D.J. Forbes. 1988. Nuclear import can be separated into distinct steps *in vitro*: nuclear binding and translocation. *Cell.* 52:641–653.

Niehrs, C., W.B. Huttner, and U Rüther. 1992. In vivo expression and stoichiometric sulfation of the artificial protein sulfophilin, a polymer of tyrosine sulfation sites. *J. Biol. Chem.* 267:15938–15942.

O'Farrell, P.H. 1975. High resolution two-dimensional electrophoresis. *J. Biol. Chem.* 250:4007–4021.

Pante, N., and U. Aebi. 1995*a.* Exploring nuclear pore complex structure and function in molecular detail. *J. Cell Sci. Suppl.* 19:1–11.

Pante, N., and U. Aebi. 1995*b.* Toward a molecular understanding of the structure and function of the nuclear pore complex. *Int. Rev. Cytol.* 162B:225–255.

Pante, N., and U. Aebi. 1996. Toward the molecular dissection of protein import into nuclei. *Curr. Opin. Cell Biol.* 8:397–406.

Pante, N., R. Bastos, B. McMorrow, B. Burke, and U. Aebi. 1994. Interaction and three-dimensional localization of a group of nuclear pore complex proteins. *J. Cell Biol.* 126:603–617.

Park, M., M. Dean, C.S. Cooper, M. Schmidt, S.J. O'Brien, D.G. Blair, and G.F. Vande Woude. 1986. Mechanism of *met* oncogene activation. *Cell.* 45:895–904.

Powers, M.A., C. Macaulay, F.R. Masiarz, and D.J. Forbes. 1995. Reconstituted nuclei depleted of a novel vertebrate GLFG nuclear pore protein, p97, import but are defective in nuclear growth and replication. *J. Cell Biol.* 128:1–9.

Radu, A., M.S. Moore, and G. Blobel. 1995. The peptide repeat domain of nucleoporin nup98 functions as a docking site in transport across the nuclear pore complex. *Cell.* 81:215–222.

Reichelt, R., A. Holzenburg, E.L. Buhle, M. Jarnik, A. Engel, and U. Aebi. 1990. Correlation between structure and mass distribution of the nuclear pore complex and of distinct pore components. *J. Cell Biol.* 110:883–894.

Richardson, W.D., A.D. Mills, S.M. Dilworth, R.A. Laskey, and C. Dingwall. 1988. Nuclear protein migration involves two steps: rapid binding at the nuclear envelope followed by slower translocation through the nuclear pores. *Cell.* 52:655–664.

Ris, H. 1989. Three-dimensional imaging of cell ultrastructure with high resolution low voltage SEM. *Inst. Phys. Conf. Ser.* 98:657–662.

Ris, H. 1991. The three dimensional structure of the nuclear pore complex as seen by high voltage electron microscopy and high resolution low voltage scanning electron microscopy. *EMSA Bull.* 21:54–56.

Ris, H., and M. Malecki. 1993. High-resolution field emission scanning electron microscope imaging of internal cell structures after epon extraction from sections: a new approach to correlative ultrastructural and immunocytochemical studies. *J. Struct. Biol.* 111:148–157.

Roth, M.B. Spheres, coiled bodies, and nuclear bodies. *Curr. Opin. Cell Biol.* 7: 325–328.

Rout, M.P., and S.R. Wente. 1994. Pores for thought: nuclear pore complex proteins. *Trends Cell Biol.* 4:357–365.

Sanger, F., S. Nicklen, and A.R. Coulson. 1977. DNA sequencing with chain-terminating inhibitors. *Proc. Natl. Acad. Sci. USA.* 74:5463–5467.

Schnölzer, M., P. Alewood, A. Jones, D. Alewood, and S.B.H. Kent. 1992. In situ neutralization in Boc-chemistry solid phase peptide synthesis. *Int. J. Peptide Protein Res.* 40:180–193.

Simos, G., and E.C. Hurt. 1995. Nucleocytoplasmic transport: factors and mechanisms. *FEBS Lett.* 369:107–112.

Soman, N.R., P. Correa, B.A. Ruiz, and G.N. Wogan. 1991. The TPR-MET oncogenic rearrangement is present and expressed in human gastric carcinoma and precursor lesions. *Proc. Natl. Acad. Sci. USA.* 88:4892–4896.

Strouboulis, J., and A.P. Wolffe. 1996. Functional compartmentalization of the nucleus. *J. Cell Sci.* 109:1991–2000.

Sukegawa, J., and G. Blobel. 1993. A nuclear pore complex protein that contains zinc finger binding motifs, binds DNA, and faces the nucleoplasm. *Cell.* 72:29–38.

Summers, M.D. 1971. Electron microscopic observations on granulosis virus entry, uncoating and replication processes during infection of the midgut cells of *Trichoplusia ni. J. Ultrastruct. Res.* 35:606–625.

Sweet, D.J., and L. Gerace. 1995. Taking from the cytoplasm and giving to the pore: soluble transport factors in nuclear protein import. *Trends Cell Biol.* 5: 444–447.

Thomas, J.O., and R.D. Kornberg. 1975. An octamer of histones in chromatin and free in solution. *Proc. Natl. Acad. Sci. USA.* 72:2626–2630.

Venetianer, A., D.L. Schiller, T. Magin, and W.W. Franke. 1983. Cessation of cytokeratin expression in a rat hepatoma cell line lacking differentiated functions. *Nature (Lond.).* 305:730–733.

Wilken, N., J.-L. Senecal, U. Scheer, and M.-C. Dabauvalle. 1995. Localization of the Ran-GTP binding protein RanBP2 at the cytoplasmic side of the nuclear pore complex. *Eur. J. Cell Biol.* 68:211–219.

Wozniak, R.W., E. Bartnik, and G. Blobel. 1989. Primary structure analysis of an integral membrane glycoprotein of the nuclear pore. *J. Cell Biol.* 108: 2083–2092.

Wu, J., M.J. Matunis, D. Kraemer, G. Blobel, and E. Coutavas. 1995. Nup358, a cytoplasmically exposed nucleoporin with peptide repeats, Ran-GTP binding sites, zinc fingers, a cyclophilin A homologous domain, and a leucine-rich region. *J. Biol. Chem.* 270:14209–14213.

Yokoyama, N., N. Hayashi, T. Seki, N. Pante, T. Ohba, K. Nishil, K. Kuma, T. Hayashida, T. Miyata, U. Aebi et al. 1995. A giant nucleopore protein that binds Ran/TC4. *Nature (Lond.).* 376:184–188.